Numerical analysis of superconducting phases in the extended Hubbard model with non-local pairing

University of Pisa, a.y. 2025-2026

Alessandro Gori*

Thesis for the Master's degree in Physics

Abstract

[To be continued...]Math font: `macro:->\protect \mathversion   cmsy8`
Main font: `cmtt9`

Contents

*a.gori23@studenti.unipi.it / nepero27178@github.com

List of symbols and abbreviations

AF	Anti-Ferromagnetic
BCS	Bardeen-Cooper-Schrieffer (theory)
DoF	Degree of Freedom
HF	Hartree-Fock
HFPs	Hartree-Fock parameters
LRT	Linear Response Theory
MFT	Mean-Field Theory
SC	Superconductor
SSB	Spontaneous Symmetry Breaking
T_c	Critical temperature

Part I

Mean-Field-Theory analysis

Chapter 1

Anti-Ferromagnetic instability

In this chapter, the effect of the non-local interaction on the antiferromagnetic phase is discussed. The MFT derivation for the Hubbard Model is discussed in App. A.

1.1 Symmetry considerations for the AF phase

[To be continued...]

1.2 Antiferromagnetism in the conventional Hubbard model

The Anti-Ferromagnetic phase, specified by the Ansatz (A.2) (which is explicitly breaking translational invariance in each spin sector, while preserving $U^z(1)$ and $U^c(1)$ symmetries) reduces the hamiltonian to the form of Eq. (A.3)

$$\hat{H}_t + \hat{H}_U \overset{\text{MFT}}{\simeq} -t \sum_{\langle \mathbf{rr'} \rangle} \sum_{\sigma} \hat{c}_{\mathbf{r}\sigma}^{\dagger} \hat{c}_{\mathbf{r'}\sigma} + nU \sum_{\mathbf{r}} [\hat{n}_{\mathbf{r}\uparrow} + \hat{n}_{\mathbf{r}\downarrow}] - mU \sum_{\mathbf{r}} (-1)^{x+y} [\hat{n}_{\mathbf{r}\uparrow} - \hat{n}_{\mathbf{r}\downarrow}]$$

In reciprocal space, the hamiltonian decomposes as in Eq. (A.5),

$$\hat{H}_t + \hat{H}_U \overset{\text{MFT}}{\simeq} \sum_{\mathbf{k} \in \text{MBZ}} \sum_{\sigma} \hat{\Psi}_{\mathbf{k}\sigma}^{\dagger} h_{\mathbf{k}\sigma} \hat{\Psi}_{\mathbf{k}\sigma} \quad \text{being} \quad h_{\mathbf{k}\sigma} \equiv \begin{bmatrix} \epsilon_{\mathbf{k}} & -\Delta_{\sigma} \\ -\Delta_{\sigma} & -\epsilon_{\mathbf{k}} \end{bmatrix}$$

and $\Delta_{\uparrow} = mU$, $\Delta_{\downarrow} = -mU$. Nambu spinorial formulation is used,

$$\hat{\Psi}_{\mathbf{k}\sigma} \equiv \begin{bmatrix} \hat{c}_{\mathbf{k}\sigma} \\ \hat{c}_{\mathbf{k}+\boldsymbol{\pi}\sigma} \end{bmatrix}$$

and the free electrons energy is simply the tight binding energy

$$\epsilon_{\mathbf{k}} = -2t \left[\cos(k_x) + \cos(k_y) \right]$$

which is spin-invariant. The MFT description of the model reduces to a gas of free "γ-fermions", described by the Nambu spinor of Eq. (A.10),

$$\hat{\Gamma}_{\mathbf{k}\sigma} = W_{\mathbf{k}\sigma} \hat{\Psi}_{\mathbf{k}\sigma} = \begin{bmatrix} \hat{\gamma}_{\mathbf{k}\sigma}^{(-)} \\ \hat{\gamma}_{\mathbf{k}\sigma}^{(+)} \end{bmatrix}$$

where

$$W_{\mathbf{k}\sigma} = \begin{bmatrix} -\sin\theta_{\mathbf{k}\sigma} & -\cos\theta_{\mathbf{k}\sigma} \\ \cos\theta_{\mathbf{k}\sigma} & -\sin\theta_{\mathbf{k}\sigma} \end{bmatrix} \quad \text{and} \quad \sin 2\theta_{\mathbf{k}\sigma} \equiv \frac{\Delta_{\sigma}}{E_{\mathbf{k}}}$$

These fermions populate the two bands $\pm E_{\mathbf{k}} = \sqrt{\epsilon_{\mathbf{k}}^2 + \Delta^2}$. The entire system is mapped onto an ensemble of pseudo-spins, each subject to a pseudo-field, as in Fig. 1.1. To diagonalize the system

essentially means to align each pseudo-spin with the z axis. Within on the notation of Fig. A.3, the following expectations values hold:

$$\langle\hat{\Psi}_{\mathbf{k}\sigma}^{\dagger}\tau^{x}\hat{\Psi}_{\mathbf{k}\sigma}\rangle = \sin(2\theta_{\mathbf{k}})\langle\hat{\Gamma}_{\mathbf{k}\sigma}^{\dagger}\tau^{z}\hat{\Gamma}_{\mathbf{k}\sigma}\rangle \tag{1.1}$$

$$\langle\hat{\Psi}_{\mathbf{k}\sigma}^{\dagger}\tau^{y}\hat{\Psi}_{\mathbf{k}\sigma}\rangle = 0 \tag{1.2}$$

$$\langle\hat{\Psi}_{\mathbf{k}\sigma}^{\dagger}\tau^{z}\hat{\Psi}_{\mathbf{k}\sigma}\rangle = -\cos(2\theta_{\mathbf{k}})\langle\hat{\Gamma}_{\mathbf{k}\sigma}^{\dagger}\tau^{z}\hat{\Gamma}_{\mathbf{k}\sigma}\rangle \tag{1.3}$$

and since the γ-fermions are free and in the rotated frame the pseudo-field points "up",

$$\langle\hat{\Gamma}_{\mathbf{k}\sigma}^{\dagger}\tau^{z}\hat{\Gamma}_{\mathbf{k}\sigma}\rangle = \frac{1}{2}\left[f\left(-E_{\mathbf{k}};\beta,\tilde{\mu}\right) - f\left(E_{\mathbf{k}};\beta,\tilde{\mu}\right)\right]$$

1.3   EHM model and antiferromagnetic ordering

Consider now the non-local interaction $\hat{H}_{V}$: since only translational invariance is broken in the AF phase, the only relevant contributions coming from Wick's decomposition are Hartree terms and the same-spin Fock term. The net effect obtained by including this interaction, as I will explain, is a renormalization of the various quantities,

$$\epsilon_{\mathbf{k}} \to \tilde{\epsilon}_{\mathbf{k}\sigma} \qquad E_{\mathbf{k}} \to \tilde{E}_{\mathbf{k}\sigma} \qquad \Delta_{\sigma} \to \tilde{\Delta}_{\mathbf{k}\sigma} \qquad \theta_{\mathbf{k}\sigma} \to \tilde{\theta}_{\mathbf{k}\sigma} \qquad W_{\mathbf{k}\sigma} \to \tilde{W}_{\mathbf{k}\sigma}$$

The band energies renormalization is simply

$$\tilde{E}_{\mathbf{k}\sigma} \equiv \sqrt{\tilde{\epsilon}_{\mathbf{k}\sigma}^{2} + |\tilde{\Delta}_{\mathbf{k}\sigma}|^{2}}$$

and the following relations hold:

$$\langle\hat{\Psi}_{\mathbf{k}\sigma}^{\dagger}\tau^{x}\hat{\Psi}_{\mathbf{k}\sigma}\rangle = \sin(2\tilde{\theta}_{\mathbf{k}})\sin(2\tilde{\zeta}_{\mathbf{k}})\langle\hat{\Gamma}_{\mathbf{k}\sigma}^{\dagger}\tau^{z}\hat{\Gamma}_{\mathbf{k}\sigma}\rangle \tag{1.4}$$

$$\langle\hat{\Psi}_{\mathbf{k}\sigma}^{\dagger}\tau^{y}\hat{\Psi}_{\mathbf{k}\sigma}\rangle = \sin(2\tilde{\theta}_{\mathbf{k}})\cos(2\tilde{\zeta}_{\mathbf{k}})\langle\hat{\Gamma}_{\mathbf{k}\sigma}^{\dagger}\tau^{z}\hat{\Gamma}_{\mathbf{k}\sigma}\rangle \tag{1.5}$$

$$\langle\hat{\Psi}_{\mathbf{k}\sigma}^{\dagger}\tau^{z}\hat{\Psi}_{\mathbf{k}\sigma}\rangle = -\cos(2\tilde{\theta}_{\mathbf{k}})\langle\hat{\Gamma}_{\mathbf{k}\sigma}^{\dagger}\tau^{z}\hat{\Gamma}_{\mathbf{k}\sigma}\rangle \tag{1.6}$$

with:

$$\sin(2\tilde{\xi}_{\mathbf{k}}) = \frac{\text{Re}\{\tilde{\Delta}_{\mathbf{k}}\}}{|\tilde{\Delta}_{\mathbf{k}}|} \qquad \cos(2\tilde{\xi}_{\mathbf{k}}) = \frac{\text{Im}\{\tilde{\Delta}_{\mathbf{k}}\}}{|\tilde{\Delta}_{\mathbf{k}}|} \qquad \sin(2\tilde{\theta}_{\mathbf{k}}) = \frac{|\tilde{\Delta}_{\mathbf{k}}|}{\tilde{E}_{\mathbf{k}}} \qquad \cos(2\tilde{\theta}_{\mathbf{k}}) = \frac{\tilde{\epsilon}_{\mathbf{k}}}{\tilde{E}_{\mathbf{k}}} \tag{1.7}$$

The physical behavior is the same as for the pure Hubbard model. In next sections the different contributions to renormalization are treated.

1.3.1   Hartree renormalization of chemical potential and gap

The same-spin and opposite-spin non-local Hartree terms are

$$\underbrace{-V\sum_{\langle ij\rangle}\sum_{\sigma}\left[\langle\hat{n}_{i\sigma}\rangle\hat{n}_{j\sigma} + \hat{n}_{i\sigma}\langle\hat{n}_{j\sigma}\rangle\right]}_{\text{s.s.}}\underbrace{-V\sum_{\langle ij\rangle}\sum_{\sigma}\left[\langle\hat{n}_{i\sigma}\rangle\hat{n}_{j\overline{\sigma}} + \hat{n}_{i\sigma}\langle\hat{n}_{j\overline{\sigma}}\rangle\right]}_{\text{o.s.}}$$

Let $i \to \mathbf{r} = (x,y)$ and $j \to \mathbf{r}' = (x',y')$. Then, using the Ansatz of Eq. (A.2), summarized as

$$\langle\hat{n}_{\mathbf{r}\sigma}\rangle = n - (-1)^{x+y+\delta_{\sigma=\uparrow}}m$$

we get

$$\overbrace{-nV\sum_{\langle\mathbf{rr}'\rangle}\sum_{\sigma}\left[\hat{n}_{\mathbf{r}'\sigma} + \hat{n}_{\mathbf{r}\sigma}\right] + mV\sum_{\langle\mathbf{rr}'\rangle}\sum_{\sigma}(-1)^{\delta_{\sigma=\uparrow}}\left[(-1)^{x'+y'}\hat{n}_{\mathbf{r}'\sigma} + (-1)^{x+y}\hat{n}_{\mathbf{r}\sigma}\right]}^{\text{s.s.}}$$

$$\underbrace{-nV\sum_{\langle\mathbf{rr}'\rangle}\sum_{\sigma}\left[\hat{n}_{\mathbf{r}'\overline{\sigma}} + \hat{n}_{\mathbf{r}\sigma}\right] + mV\sum_{\langle\mathbf{rr}'\rangle}\sum_{\sigma}\left[(-1)^{x'+y'+\delta_{\overline{\sigma}=\uparrow}}\hat{n}_{\mathbf{r}'\overline{\sigma}} + (-1)^{x+y+\delta_{\sigma=\uparrow}}\hat{n}_{\mathbf{r}\sigma}\right]}_{\text{o.s.}}$$
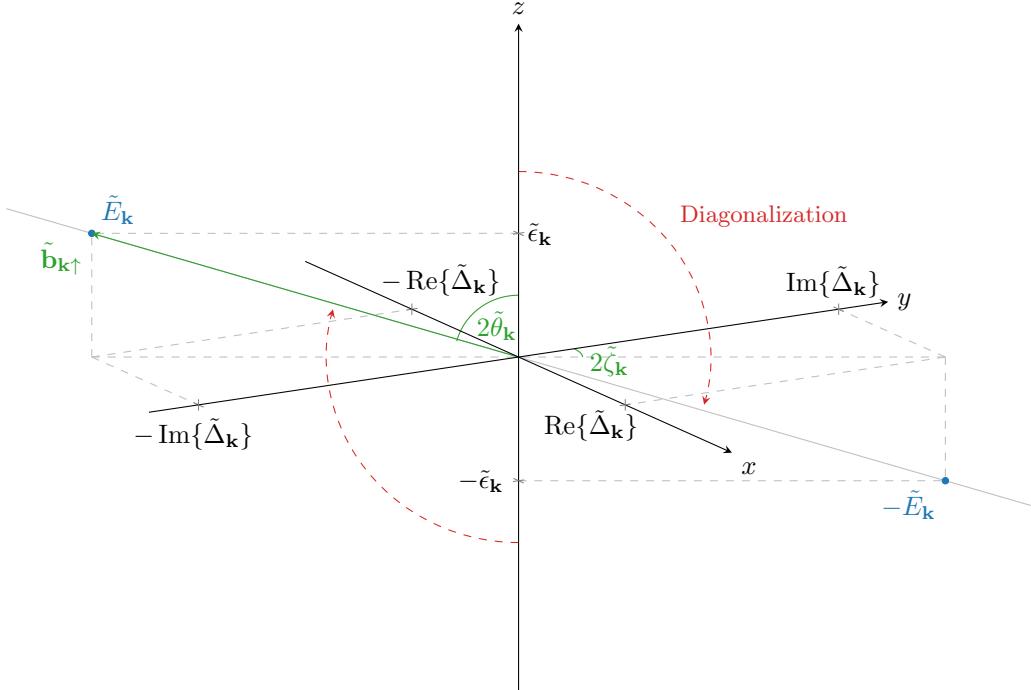
Figure 1.1 Sketch of the diagonalization of the pseudo-spin problem. The dashed line represents the diagonalization given by the z-axis alignment with the field direction. In the top-right side of the picture are listed the expectation values of the original Nambu spinor.

For a square lattice, if $\mathbf{r} = (x, y)$ and $\mathbf{r}' = (x', y')$ are NNs evidently

$$(-1)^{x'+y'} = (-1)^{x+y+1}$$

Moreover,

$$(-1)^{\delta_{\overline{\sigma}=\uparrow}} = (-1)^{\delta_{\sigma=\uparrow}+1}$$

We obtain

$$\overbrace{-nV \sum_{\langle \mathbf{rr}' \rangle} \sum_{\sigma} [\hat{n}_{\mathbf{r}\sigma} + \hat{n}_{\mathbf{r}'\sigma}]}^{\text{s.s. (density)}} + \overbrace{mV \sum_{\langle \mathbf{rr}' \rangle} \sum_{\sigma} (-1)^{x+y+\delta_{\sigma=\uparrow}} [\hat{n}_{\mathbf{r}\sigma} - \hat{n}_{\mathbf{r}'\sigma}]}^{\text{s.s. (magnetization)}}$$

$$\underbrace{-nV \sum_{\langle \mathbf{rr}' \rangle} \sum_{\sigma} [\hat{n}_{\mathbf{r}\sigma} + \hat{n}_{\mathbf{r}'\overline{\sigma}}]}_{\text{o.s. (density)}} + \underbrace{mV \sum_{\langle \mathbf{rr}' \rangle} \sum_{\sigma} (-1)^{x+y+\delta_{\sigma=\uparrow}} [\hat{n}_{\mathbf{r}\sigma} + \hat{n}_{\mathbf{r}'\overline{\sigma}}]}_{\text{o.s. (magnetization)}} \quad (1.8)$$

In the above expressions the various contribution have been separated in "density" contributions and "magnetization" contributions. Let me deal with these separately.

Density terms.   Consider the *s.s.* and *o.s.* (density) terms of Expr. (1.8). Since

$$\sum_{\langle \mathbf{rr}' \rangle} \sum_{\sigma} [\hat{n}_{\mathbf{r}\sigma} + \hat{n}_{\mathbf{r}'\sigma}] = \sum_{\langle \mathbf{rr}' \rangle} \sum_{\sigma} [\hat{n}_{\mathbf{r}\sigma} + \hat{n}_{\mathbf{r}'\overline{\sigma}}] = z\hat{N}$$

with $z = 4$ the lattice coordination factor, indicating the number of NNs per site, then the first and third terms of Expr. (1.8) contribute to a pure chemical potential shift. The renormalized chemical potential is:

$$\tilde{\mu} \equiv \mu + 2znV \quad (1.9)$$

Magnetization terms.   The s.s. and o.s. (magnetization) terms of Expr. (1.8) are to be reduced to a renormalization of the gap function. Explicitly,

$$mV \sum_{\langle \mathbf{rr'} \rangle} \sum_{\sigma} (-1)^{x+y+\delta_{\sigma=\uparrow}} \left[\hat{n}_{\mathbf{r}\sigma} - \hat{n}_{\mathbf{r'}\sigma} \right] + mV \sum_{\langle \mathbf{rr'} \rangle} \sum_{\sigma} (-1)^{x+y+\delta_{\sigma=\uparrow}} \left[\hat{n}_{\mathbf{r}\sigma} + \hat{n}_{\mathbf{r'}\bar{\sigma}} \right]$$

$$= -2zmV \sum_{\mathbf{r}} (-1)^{x+y} \left[\hat{n}_{\mathbf{r}\uparrow} - \hat{n}_{\mathbf{r}\downarrow} \right] \quad (1.10)$$

Consider now the last term of the pure Hubbard model under MFT approximations of Eq. (A.3),

$$-mU \sum_{\mathbf{r}} (-1)^{x+y} \left[\hat{n}_{\mathbf{r}\uparrow} - \hat{n}_{\mathbf{r}\downarrow} \right] \quad \text{(Local gap)}$$

Expr. (1.10) is formally identical, thus we obtain a contribution to the renormalization of the AF gap,

$$\Delta \to \Delta + 2zmV + \text{(s.s. contribution)} \quad (1.11)$$

This, together with Eq. (1.9), concludes the non-local Hartree reparametrization of the hamiltonian. Next section is devoted to analyzing the effect of the Fock term.

1.3.2   Fock renormalization of the hopping amplitude

From Wick's decomposition of $\hat{H}_V$, the only allowed Fock term comes from the same-spin part due to SU(2) symmetry selection rules. Said hamiltonian term is

$$V \sum_{\langle ij \rangle} \sum_{\sigma} \left[\langle \hat{c}_{i\sigma}^{\dagger} \hat{c}_{j\sigma} \rangle \hat{c}_{j\sigma}^{\dagger} \hat{c}_{i\sigma} + \text{h.c.} \right] \quad (1.12)$$

(note the + sign in front of it). A bond-wise hopping amplitude can be defined,

$$\tilde{t}_{ij\sigma} \equiv t - V \langle \hat{c}_{j\sigma}^{\dagger} \hat{c}_{i\sigma} \rangle$$

In the AF phase, given some site i and a spin σ, evidently $\tilde{t}_{ij\sigma}$ must be identical for any NN site j. Over the planar square lattice, this implies that the quantity $\langle \hat{c}_{j\sigma}^{\dagger} \hat{c}_{i\sigma} \rangle$ exhibits s^*-wave symmetry (also referred to as "Extended s-wave symmetry"). Later in the text, different symmetry structures will be discussed thoroughly. For now, the s^*-wave symmetry is the one given in Tab. **??** and depicted in Fig. **??**. These considerations will become useful later. The effective diffusive hamiltonian is given by

$$\hat{H}_{\tilde{t}} = \hat{H}_t + V \sum_{\langle ij \rangle} \sum_{\sigma} \left[\langle \hat{c}_{i\sigma}^{\dagger} \hat{c}_{j\sigma} \rangle \hat{c}_{j\sigma}^{\dagger} \hat{c}_{i\sigma} + \text{h.c.} \right]$$

$$= -\sum_{\langle ij \rangle} \sum_{\sigma} \left[\tilde{t}_{ij\sigma} \hat{c}_{i\sigma}^{\dagger} \hat{c}_{j\sigma} + \text{h.c.} \right]$$

As will become clear in next section, not only the diffusive part of the hamiltonian actually is affected by the Fock renormalization; also the gap terms are effectively renormalized.

In reciprocal space, the effective hopping must be transformed as well. Consider the Fourier Transform given in Eq. (**??**), applied to Eq. (1.12),

$$V \sum_{\langle ij \rangle} \sum_{\sigma} \left[\langle \hat{c}_{i\sigma}^{\dagger} \hat{c}_{j\sigma} \rangle \hat{c}_{j\sigma}^{\dagger} \hat{c}_{i\sigma} + \text{h.c.} \right]$$

$$= \frac{2V}{L_x L_y} \sum_{\mathbf{K}, \mathbf{k}, \mathbf{k'}} \sum_{\sigma} \left[\cos\left(\delta k_x\right) + \cos\left(\delta k_y\right) \right] \langle \hat{c}_{\mathbf{K}+\mathbf{k}\sigma}^{\dagger} \hat{c}_{\mathbf{K}-\mathbf{k'}\sigma} \rangle \hat{c}_{\mathbf{K}-\mathbf{k}\sigma}^{\dagger} \hat{c}_{\mathbf{K}+\mathbf{k'}\sigma} \quad (1.13)$$

where the 2 prefactor comes from recognizing that the h.c. generates an identical contribution to the full sum. In order to proceed, it is now necessary to understand how the AF phase is realized in reciprocal space. As is exposed in App. A, to impose an AF Ansatz of the form

$$\langle \hat{n}_{\mathbf{r}\sigma} \rangle = n - (-1)^{x+y+\delta_{\sigma=\uparrow}} m$$

a │ Generic vectors.   b │ Change of variables.
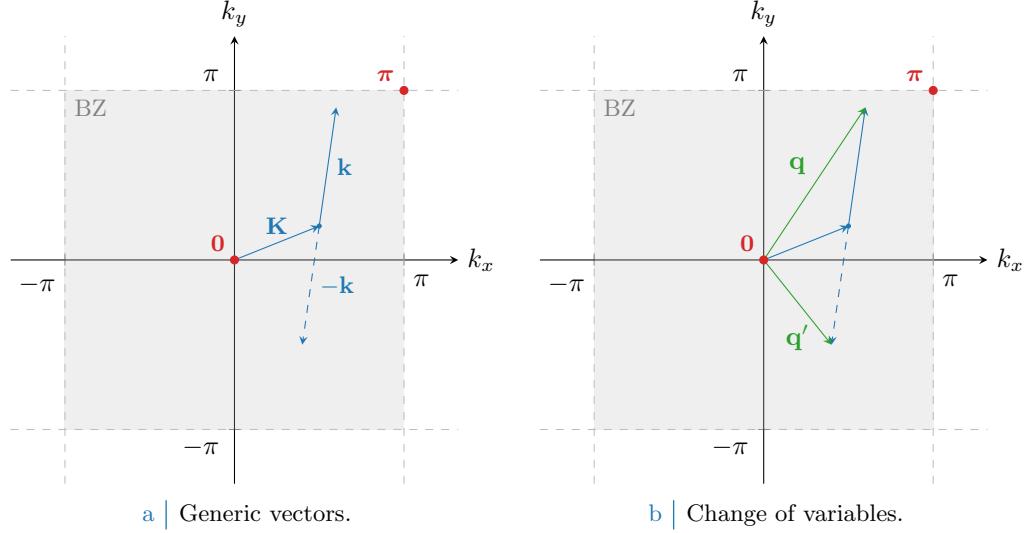
Figure 1.2 │ Representation of the vectors involved in the diagonal terms of Eq. (1.14). In Fig. 1.2a generic vectors are considered, cycling over all values of $\mathbf{K}, \mathbf{k} \in$ BZ. In Fig. 1.2b is depicted the variables change to the new vectors $\mathbf{q}, \mathbf{q}'$.

leads to an AF ground-state of free fermions at temperature β described by the Nambu spinor of Eq. (A.10). All parameters are renormalized, thus we must account for renormalized band energies $\pm \tilde{E}_{\mathbf{k}\sigma}$ as well. The ground-state is realized by simply populating the two bands $\pm \tilde{E}_{\mathbf{k}\sigma}$ as

$$\bigotimes_{\mathbf{k}\in\mathrm{MBZ}} \bigotimes_{\sigma} \left[\left(\hat{\gamma}_{\mathbf{k}\sigma}^{(-)}\right)^{\dagger} f(-\tilde{E}_{\mathbf{k}}; \beta, \mu) + \left(\hat{\gamma}_{\mathbf{k}\sigma}^{(+)}\right)^{\dagger} f(\tilde{E}_{\mathbf{k}}; \beta, \mu) \right] |\Omega\rangle$$

The $\hat{\gamma}$ operators are normalized superpositions of two $\hat{c}$ operators at points in reciprocal space separated by a $\boldsymbol{\pi}$ shift. It follows that the above state is ultimately a superposition of many-body pure states, each of which has either the $\mathbf{k}\sigma$ state occupied *or* the $\mathbf{k} + \boldsymbol{\pi}\sigma$ state for each $\mathbf{k} \in$ MBZ, $\sigma \in \{\uparrow, \downarrow\}$. It follows that, when computing generically $\langle \hat{c}_{\mathbf{k}_1\sigma}^{\dagger} \hat{c}_{\mathbf{k}_2\sigma} \rangle$, such expectation value can be non-zero if and only if $\mathbf{k}_1 = \mathbf{k}_2 + n\boldsymbol{\pi}$, being $n \in \mathbb{Z}$. Going back to Eq. (1.13), this implies only two contributions are non-zero:

$$\mathbf{k} = -\mathbf{k}' \quad \text{or} \quad \mathbf{k} + \boldsymbol{\pi} = -\mathbf{k}'$$

Then Eq. (1.13) is reduced to:

$$\frac{2V}{L_x L_y} \sum_{\mathbf{K}, \mathbf{k}} \sum_{\sigma} \left[\cos(2k_x) + \cos(2k_y) \right]$$

$$\left[\underbrace{\langle \hat{c}_{\mathbf{K}+\mathbf{k}\sigma}^{\dagger} \hat{c}_{\mathbf{K}+\mathbf{k}\sigma} \rangle \hat{c}_{\mathbf{K}-\mathbf{k}\sigma}^{\dagger} \hat{c}_{\mathbf{K}-\mathbf{k}\sigma}}_{\text{Diagonal terms}} - \underbrace{\langle \hat{c}_{\mathbf{K}+\mathbf{k}\sigma}^{\dagger} \hat{c}_{\mathbf{K}+\mathbf{k}+\boldsymbol{\pi}\sigma} \rangle \hat{c}_{\mathbf{K}-\mathbf{k}\sigma}^{\dagger} \hat{c}_{\mathbf{K}-\mathbf{k}-\boldsymbol{\pi}\sigma}}_{\text{Off-diagonal terms}} \right] \quad (1.14)$$

Now, the above equation presents *diagonal* and *off-diagonal* terms. Let me discuss them separately.

Diagonal terms. The diagonal terms of Eq. (1.14) are simple density interactions with the mean density field. Consider Fig. 1.2a: density at vector $\mathbf{q} \equiv \mathbf{K} + \mathbf{k}$ interacts with the mean density at vector $\mathbf{q}' \equiv \mathbf{K} - \mathbf{k}$. These variables are depicted in Fig. 1.2b. Apply the variable change in the diagonal part of Eq. (1.14),

$$\frac{2V}{L_x L_y} \sum_{\mathbf{q}, \mathbf{q}'} \sum_{\sigma} \left[\cos(2k_x) + \cos(2k_y) \right] \langle \hat{c}_{\mathbf{K}+\mathbf{k}\sigma}^{\dagger} \hat{c}_{\mathbf{K}+\mathbf{k}\sigma} \rangle \hat{c}_{\mathbf{K}-\mathbf{k}\sigma}^{\dagger} \hat{c}_{\mathbf{K}-\mathbf{k}\sigma}$$

$$= \frac{2V}{L_x L_y} \sum_{\mathbf{q}, \mathbf{q}'} \sum_{\sigma} \left[\cos(\delta q_x) + \cos(\delta q_y) \right] \langle \hat{c}_{\mathbf{q}\sigma}^{\dagger} \hat{c}_{\mathbf{q}\sigma} \rangle \hat{c}_{\mathbf{q}'\sigma}^{\dagger} \hat{c}_{\mathbf{q}'\sigma} \quad (1.15)$$

being for $\ell = x, y$

$$\begin{aligned}\delta q_\ell &\equiv q_\ell - q'_\ell \\ &= (K_\ell + k_\ell) - (K_\ell - k_\ell) \\ &= 2k_\ell\end{aligned}$$

The form factor $\cos(\delta q_x) + \cos(\delta q_y)$ decomposes in waves as in Eq. (**??**). In the AF phase, $\langle \hat{c}^\dagger_{\mathbf{q}\sigma} \hat{c}_{\mathbf{q}\sigma} \rangle$ must be s^*-wave symmetric, as anticipated in the starting discussion of Sec. 1.3.2. This is due to the fact that of the four symmetries listed above, only the first one exhibits both x, y reflections symmetry and $\pi/2$ rotational invariance. It follows, only the s^*-wave component when coupled to $\langle \hat{c}^\dagger_{\mathbf{q}\sigma} \hat{c}_{\mathbf{q}\sigma} \rangle$ in Eq. (1.15) gives a non-null contribution, reducing the latter to

$$\frac{2V}{L_x L_y} \sum_{\mathbf{q},\mathbf{q}'} \sum_\sigma \left[\cos(\delta q_x) + \cos(\delta q_y)\right] \langle \hat{c}^\dagger_{\mathbf{q}\sigma} \hat{c}_{\mathbf{q}\sigma} \rangle \hat{c}^\dagger_{\mathbf{q}'\sigma} \hat{c}_{\mathbf{q}'\sigma}$$

$$= \frac{V}{L_x L_y} \sum_{\mathbf{q}'\sigma} \left(\cos q'_x + \cos q'_y\right) \hat{c}^\dagger_{\mathbf{q}'\sigma} \hat{c}_{\mathbf{q}'\sigma} \sum_{\mathbf{q}} \left(\cos q_x + \cos q_y\right) \langle \hat{c}^\dagger_{\mathbf{q}\sigma} \hat{c}_{\mathbf{q}\sigma} \rangle \quad (1.16)$$

Note that, for two vectors separated by a $\boldsymbol{\pi}$ shift,

$$\cos q_x + \cos q_y = -\cos(q_x + \pi) - \cos(q_y + \pi)$$

Because of this feature, changing the variables names $\mathbf{q}' \to \mathbf{k}$, $\mathbf{q} \to \mathbf{k}'$ for the sake of general aesthetic coherence, it becomes evident that the above equation gives the bands renormalization:

$$\epsilon_{\mathbf{k}} \equiv -2t \left(\cos k_x + \cos k_y\right)$$

$$\tilde{\epsilon}_{\mathbf{k}} \equiv \epsilon_{\mathbf{k}} + \left[\frac{1}{2L_x L_y} \sum_{\mathbf{k}'} \left(\cos k'_x + \cos k'_y\right) \langle \hat{c}^\dagger_{\mathbf{k}'\sigma} \hat{c}_{\mathbf{k}'\sigma} \rangle \right] \times 2V \left(\cos k_x + \cos k_y\right)$$

Note that on the left-hand side $\tilde{\epsilon}_{\mathbf{k}}$ is independent of σ. To explain this, let:

$$w^{(\mathbf{0})}_\sigma \equiv \frac{1}{2L_x L_y} \sum_{\mathbf{k} \in \text{BZ}} \left(\cos k_x + \cos k_y\right) \langle \hat{c}^\dagger_{\mathbf{k}\sigma} \hat{c}_{\mathbf{k}\sigma} \rangle$$

By simple symmetry considerations, it must be $\langle \hat{c}^\dagger_{\mathbf{k}\uparrow} \hat{c}_{\mathbf{k}\uparrow} \rangle = \langle \hat{c}^\dagger_{\mathbf{k}\downarrow} \hat{c}_{\mathbf{k}\downarrow} \rangle$ (as is later seen explicitly). Then,

$$w^{(\mathbf{0})}_\uparrow = w^{(\mathbf{0})}_\downarrow \equiv w^{(\mathbf{0})}$$

The computation can be simplified:

$$\begin{aligned} w^{(\mathbf{0})} &= \frac{1}{2L_x L_y} \sum_{\mathbf{k} \in \text{BZ}} \left(\cos k_x + \cos k_y\right) \langle \hat{c}^\dagger_{\mathbf{k}\uparrow} \hat{c}_{\mathbf{k}\uparrow} \rangle \\ &= \frac{1}{2L_x L_y} \sum_{\mathbf{k} \in \text{MBZ}} \left(\cos k_x + \cos k_y\right) \langle \hat{c}^\dagger_{\mathbf{k}\uparrow} \hat{c}_{\mathbf{k}\uparrow} - \hat{c}^\dagger_{\mathbf{k}+\boldsymbol{\pi}\uparrow} \hat{c}_{\mathbf{k}+\boldsymbol{\pi}\uparrow} \rangle \\ &= \frac{1}{2L_x L_y} \sum_{\mathbf{k} \in \text{MBZ}} \left(\cos k_x + \cos k_y\right) \langle \hat{\Psi}^\dagger_{\mathbf{k}\uparrow} \tau^z \hat{\Psi}_{\mathbf{k}\uparrow} \rangle \\ &= -\frac{1}{4L_x L_y} \sum_{\mathbf{k} \in \text{MBZ}} \left(\cos k_x + \cos k_y\right) \frac{\tilde{\epsilon}_{\mathbf{k}}}{\tilde{E}_{\mathbf{k}}} \left[f\left(-\tilde{E}_{\mathbf{k}}; \beta, \tilde{\mu}\right) - f\left(\tilde{E}_{\mathbf{k}}; \beta, \tilde{\mu}\right)\right] \quad (1.17) \end{aligned}$$

where in the second passage the sign change is due to the presence of the structure factor, and in the fourth passage Eq. (1.6) and the relations (1.7) have been used. It follows, finally, that the hopping parameter gets effectively renormalized:

$$\tilde{t} \equiv t - w^{(\mathbf{0})} V \quad (1.18)$$

The full effective MFT hamiltonian is spin-independent, then similarly the renormalized parameters cannot exhibit spin dependency. This justifies the fact that $\tilde{t}$ is spin-independent, and so is $\tilde{\epsilon}_{\mathbf{k}}$.

Off-diagonal terms. Consider the off-diagonal terms of Eq. (1.14). These contribute instead to the gap renormalization, being out of diagonal in the 2×2 hamiltonian matrix. Define $\mathbf{q}$, $\mathbf{q}'$ as in Fig. 1.2b, and rewrite

$$-\frac{2V}{L_x L_y} \sum_{\mathbf{K},\mathbf{k}} \sum_{\sigma} [\cos(2k_x) + \cos(2k_y)] \langle \hat{c}^\dagger_{\mathbf{K}+\mathbf{k}\sigma} \hat{c}_{\mathbf{K}+\mathbf{k}+\boldsymbol{\pi}\sigma} \rangle \hat{c}^\dagger_{\mathbf{K}-\mathbf{k}\sigma} \hat{c}_{\mathbf{K}-\mathbf{k}-\boldsymbol{\pi}\sigma}$$

$$= -\frac{2V}{L_x L_y} \sum_{\mathbf{q}} \langle \hat{c}^\dagger_{\mathbf{q}\sigma} \hat{c}_{\mathbf{q}+\boldsymbol{\pi}\sigma} \rangle \sum_{\mathbf{q}'\sigma} [\cos(\delta q_x) + \cos(\delta q_y)] \hat{c}^\dagger_{\mathbf{q}'\sigma} \hat{c}_{\mathbf{q}'+\boldsymbol{\pi}\sigma}$$

Identical considerations about the s^*-wave symmetry structure of the expectation value $\langle \hat{c}^\dagger_{\mathbf{q}\sigma} \hat{c}_{\mathbf{q}+\boldsymbol{\pi}\sigma} \rangle$ as in the above paragraph hold. Once again renaming the variables $\mathbf{q}' \to \mathbf{k}$, $\mathbf{q} \to \mathbf{k}'$ for the sake of general aesthetic coherence, this gives

$$-\frac{2V}{L_x L_y} \sum_{\mathbf{K},\mathbf{k}} \sum_{\sigma} [\cos(2k_x) + \cos(2k_y)] \langle \hat{c}^\dagger_{\mathbf{K}+\mathbf{k}\sigma} \hat{c}_{\mathbf{K}+\mathbf{k}+\boldsymbol{\pi}\sigma} \rangle \hat{c}^\dagger_{\mathbf{K}-\mathbf{k}\sigma} \hat{c}_{\mathbf{K}-\mathbf{k}-\boldsymbol{\pi}\sigma}$$

$$= -2V \left[\frac{1}{2L_x L_y} \sum_{\mathbf{k}'} \left(\cos k'_x + \cos k'_y \right) \langle \hat{c}^\dagger_{\mathbf{k}'\sigma} \hat{c}_{\mathbf{k}'+\boldsymbol{\pi}\sigma} \rangle \right] \sum_{\mathbf{k}\sigma} \left(\cos k_x + \cos k_y \right) \hat{c}^\dagger_{\mathbf{k}\sigma} \hat{c}_{\mathbf{k}+\boldsymbol{\pi}\sigma} \quad (1.19)$$

Because of this, the x component of the pseudo-magnetic field – the gap already renormalized by Eq. (1.11) when analyzing o.s. terms – takes up another renormalization contribution, finally giving

$$\tilde{\Delta}_{\mathbf{k}\sigma} \equiv m(U + 2zV) \times (-1)^{\delta_{\sigma=\uparrow}} + i2V w_\sigma^{(\boldsymbol{\pi})} \left(\cos k_x + \cos k_y \right) \quad (1.20)$$

where

$$w_\sigma^{(\boldsymbol{\pi})} \equiv -\frac{i}{2L_x L_y} \sum_{\mathbf{k}\in\text{BZ}} \left(\cos k_x + \cos k_y \right) \langle \hat{c}^\dagger_{\mathbf{k}\sigma} \hat{c}_{\mathbf{k}+\boldsymbol{\pi}\sigma} \rangle$$

As will be clear in few lines, $w_\sigma^{(\boldsymbol{\pi})}$ as is defined here is purely real (due to the presence of a $-i$ prefactor). This makes $\tilde{\Delta}_{\mathbf{k}\sigma}$ made of two contributions,

$$\text{Re}\{\tilde{\Delta}_{\mathbf{k}\sigma}\} = m(U + 2zV) \times (-1)^{\delta_{\sigma=\uparrow}} \qquad \text{Im}\{\tilde{\Delta}_{\mathbf{k}\sigma}\} = 2V w_\sigma^{(\boldsymbol{\pi})} \left(\cos k_x + \cos k_y \right)$$

Now, since the gapped band value cannot depend on the spin index for symmetry reasons,

$$\tilde{E}_{\mathbf{k}} = \sqrt{\tilde{\epsilon}_{\mathbf{k}}^2 + |\tilde{\Delta}_{\mathbf{k}\sigma}|^2}$$

this implies necessarily $|\tilde{\Delta}_{\mathbf{k}\uparrow}| = |\tilde{\Delta}_{\mathbf{k}\downarrow}|$. This is possible either if $w_\uparrow^{(\boldsymbol{\pi})} = \pm w_\downarrow^{(\boldsymbol{\pi})}$. Actually, in the end the exact sign does not matter: all that matters is the gap amplitude $|\tilde{\Delta}_{\mathbf{k}\sigma}|$, thus we may restrict to $\sigma = \uparrow$ and omit from now on the spin index. [Not so sure about this.]. This then gives us the final result for the renormalized gap function,

$$\tilde{\Delta}_{\mathbf{k}} \equiv m(U + 2zV) + 2iw^{(\boldsymbol{\pi})}V \left(\cos k_x + \cos k_y \right) \quad (1.21)$$

This result, together with Eqns. (1.9) and (1.18), concludes the renormalization of all parameters due to the non-local interaction. To calculate $w^{(\boldsymbol{\pi})}$ self consistently, we may use:

$$w^{(\boldsymbol{\pi})} = -\frac{i}{2L_x L_y} \sum_{\mathbf{k}\in\text{BZ}} \left(\cos k_x + \cos k_y \right) \langle \hat{c}^\dagger_{\mathbf{k}\uparrow} \hat{c}_{\mathbf{k}+\boldsymbol{\pi}\uparrow} \rangle$$

$$= -\frac{i}{2L_x L_y} \sum_{\mathbf{k}\in\text{MBZ}} \left(\cos k_x + \cos k_y \right) \langle \hat{c}^\dagger_{\mathbf{k}\uparrow} \hat{c}_{\mathbf{k}+\boldsymbol{\pi}\uparrow} - \hat{c}^\dagger_{\mathbf{k}+\boldsymbol{\pi}\uparrow} \hat{c}_{\mathbf{k}\uparrow} \rangle$$

$$= \frac{1}{2L_x L_y} \sum_{\mathbf{k}\in\text{MBZ}} \left(\cos k_x + \cos k_y \right) \langle \hat{\Psi}^\dagger_{\mathbf{k}\uparrow} \tau^y \hat{\Psi}_{\mathbf{k}\uparrow} \rangle$$

$$= \frac{1}{4L_x L_y} \sum_{\mathbf{k}\in\text{MBZ}} \left(\cos k_x + \cos k_y \right) \frac{\text{Im}\{\tilde{\Delta}_{\mathbf{k}}\}}{\tilde{E}_{\mathbf{k}}} \left[f\left(-\tilde{E}_{\mathbf{k}}; \beta, \tilde{\mu} \right) - f\left(\tilde{E}_{\mathbf{k}}; \beta, \tilde{\mu} \right) \right] \quad (1.22)$$

Notice that this expression is purely real, as promised, and contributes to the y component of the pseudo-field of Fig. 1.1.

1.3.3   Renormalized hamiltonian behavior

Summing up, the non-local interaction $\hat{H}_V$ when discussed within MFT affects the EHM hamiltonian by renormalizing the various parameters as:

$$\tilde{\mu} \equiv \mu + 2znV$$

$$\tilde{t} \equiv t - w^{(\mathbf{0})}V$$

$$\tilde{\Delta}_{\mathbf{k}} \equiv m(U + 2zV) + 2iw^{(\boldsymbol{\pi})}V\left[\cos\left(k_x\right) + \cos\left(k_y\right)\right]$$

Various details are to be noted. First, the non-local interaction both contributes by enlarging the real part of the gap [To be understood: why does a non-local attraction increase the gap?] as well as introducing a s^*-wave shaped imaginary gap. Interestingly, if

$$\left(w^{(\mathbf{0})}\right)^{-1} = V/t$$

the diffusive part of the hamiltonian drops to zero. For even larger values, diffusion becomes energetically expensive and V-induced localization appears.

The new set of Hartree-Fock parameters to be determined is given by the vector

$$\mathbf{v} \equiv \begin{bmatrix} m \\ w^{(\mathbf{0})} \\ w^{(\boldsymbol{\pi})} \end{bmatrix}$$

Its three components are self-consistently determined by Eqns. (1.17) and (1.22). The self-consistent equation for m comes from Eq. (A.16), and reads

$$\begin{aligned}
m &= \frac{1}{2L_xL_y} \sum_{\mathbf{k}\in\text{BZ}} \langle \hat{c}^{\dagger}_{\mathbf{k}\uparrow}\hat{c}_{\mathbf{k}+\boldsymbol{\pi}\uparrow} - \hat{c}^{\dagger}_{\mathbf{k}\downarrow}\hat{c}_{\mathbf{k}+\boldsymbol{\pi}\downarrow}\rangle \\
&= \frac{1}{2L_xL_y} \sum_{\mathbf{k}\in\text{MBZ}} \langle \hat{\Psi}^{\dagger}_{\mathbf{k}\uparrow}\tau^x\hat{\Psi}_{\mathbf{k}\uparrow} - \hat{\Psi}^{\dagger}_{\mathbf{k}\downarrow}\tau^x\hat{\Psi}_{\mathbf{k}\downarrow}\rangle \\
&= \frac{1}{L_xL_y} \sum_{\mathbf{k}\in\text{MBZ}} \langle \hat{\Psi}^{\dagger}_{\mathbf{k}\uparrow}\tau^x\hat{\Psi}_{\mathbf{k}\uparrow}\rangle \\
&= \frac{1}{2L_xL_y} \sum_{\mathbf{k}\in\text{MBZ}} \frac{\text{Re}\{\tilde{\Delta}_{\mathbf{k}}\}}{\tilde{E}_{\mathbf{k}}} \left[f\left(-\tilde{E}_{\mathbf{k}};\beta,\tilde{\mu}\right) - f\left(\tilde{E}_{\mathbf{k}};\beta,\tilde{\mu}\right) \right]
\end{aligned} \tag{1.23}$$

In the second passage $\langle \hat{\Psi}^{\dagger}_{\mathbf{k}\uparrow}\tau^x\hat{\Psi}_{\mathbf{k}\uparrow}\rangle = -\langle \hat{\Psi}^{\dagger}_{\mathbf{k}\downarrow}\tau^x\hat{\Psi}_{\mathbf{k}\downarrow}\rangle$ has been used. In the third passage, relations (1.7) were inserted. The algorithm sketched in Sec. A.3.7 remains essentially identical, with the *caveat* of defining three HF parameters, running for each a convergence analysis.

1.4   Stability of the AF phase

The discussion above is formally correct and self-consistent, thus a HF algorithm can be sketched to extract the HFPs. However we cannot proceed without considering the instability effects of Sec. A.3.6. As is known (and we would have liked to notice earlier) the AF-SSB at wavevector $\boldsymbol{\pi}$ we are studying here, responsible of halving the BZ down to the MBZ, can produce a stable phase on pure Hubbard lattices only at half filling [**singh1990collective**]. For the EHM the situation is even worse than that: repeating the simple Linear Reponse Theory (LRT) computations of Sec. A.3.6 and mimicking Eq. (A.17), we get a proper response function

$$\tilde{\chi}_{\hat{\mathbf{S}}-\hat{\mathbf{S}}+}(\mathbf{k},\omega) = \frac{\chi_{\hat{\mathbf{S}}-\hat{\mathbf{S}}+}(\mathbf{k},\omega)}{1 - \left[U - 2V\left(\cos k_x + \cos k_y\right)\right]\chi_{\hat{\mathbf{S}}-\hat{\mathbf{S}}+}(\mathbf{k},\omega)} \tag{1.24}$$

[Double check the red part and conclude this paragraph...].

As is well documented in literature [**wietek2021stripes**], AF can establish in a wide range of spatial structures with particular shapes, for example stripes. In order to extract the precise AF phase, we should
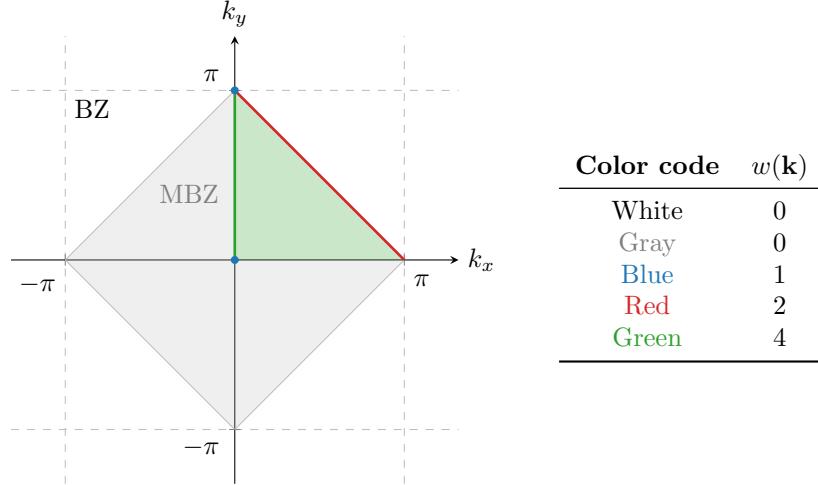
Figure 1.3 │ Graphic rendition of s^*-wave symmetry over the MBZ employed to optimize calculations. The right-side table indicates, for any point in BZ, the relative weight assigned to calculation.

1. Choose an initializer wavevector, say $\mathbf{k} = \boldsymbol{\pi}$;

2. Solve self-consistently for the HFPs at $\mathbf{k}$;

3. Compute the free energy F as a functional of the wavevector around $\mathbf{k}$;

4. Look for gradient descent of the free energy, $\boldsymbol{\nabla} F < 0$;

5. If the gradient descent is found, update $\mathbf{k} \to \mathbf{k} + \delta\mathbf{k}$ and repeat from step 2, otherwise halt.

Of course the sketched procedure can lead to a lot of complications, first the fact that at incommensurate wavevector $\mathbf{k} \neq \boldsymbol{\pi}$ the unit cell is not as simple as a pair of sites, but can become much larger requiring more refined computational solutions.

In this text we will show the self consistent result for AF-SSB at wavevector $\boldsymbol{\pi}$ even at finite doping as a first step in the above sketched procedure. The presented results are self-consistent, but unfortunately deeply unstable and unphysical at finite doping, a situation where an incommensurate and insulating AF phase is preferred to this commensurate metallic counterpart. Nevertheless we present them anyway.

1.5   HF algorithm, computational strategy and results

This section is devoted to the discussion of the self-consistent results we obtained running an iterative HF algorithm in the parameters space. As said earlier, not all presented results are in fact stable; however we decided to show them as sketch of the first step in a general self-consistent algorithm in search of the stablest AF structure.

1.5.1   Preliminary symmetry considerations

A very important feature when dealing with optimization is recognizing the complete s^* symmetry of the model, and the HFP parameters with relative self-consistency equations. Consider Eqns. (1.23), (1.17) and (1.22): in all of three the term inside the sum exhibits s^*-wave symmetry and is summed over the MBZ. Then there is no need of sweeping the entirety of the MBZ, it suffices to sweep just one fourth and just multiply coherently the result.

A little care is necessary when dealing with borders, due to MBZ nesting. Consider in fact the MBZ rhombus, sketched in gray in Fig. 1.3: due to periodicity, two of its four boundaries must be excluded from computation in order to avoid redundancy. Let those be the lower boundaries,

$$k_y = |k_x| - \pi$$

a | Non-local attraction V/t de- b | Doping $\delta = n - 0.5$ depen-
pencence.   dence.
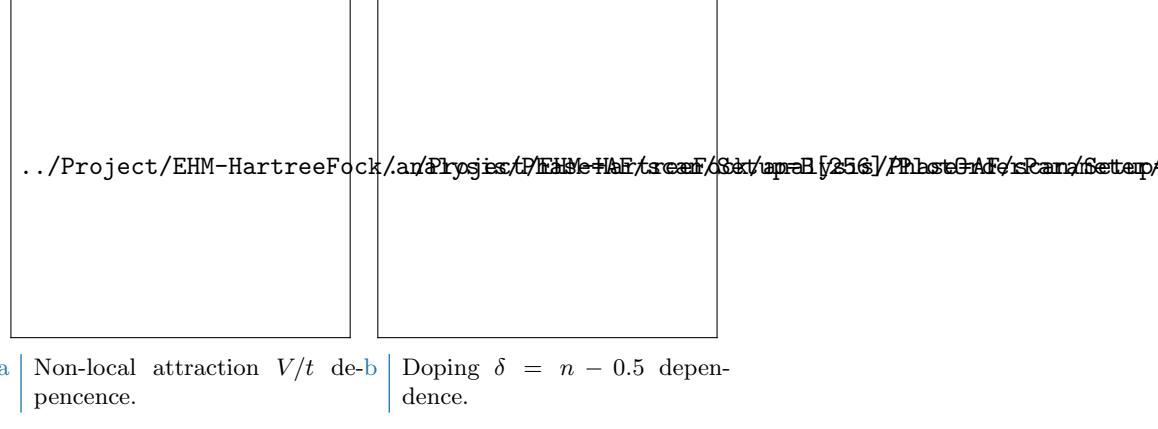
Figure 1.4 | Plots of the magnetization m in the antiferromagnetic phase as a function of both the
non-local attraction V/t (Fig. 1.4a) and the doping $\delta = n - 1/2$ (Fig. 1.4b), at fixed
local repulsion $U/t = 4$. As discussed in text, actually only $\delta = 0$ simulations are
stable.

Due to periodicity, the remaining upper boundaries lead to identical results, thus we may compute
just one of them and multiply the result by 2. In doing this, we need to avoid the edges: due to
nesting of the MBZ, the three points

$$(0, \pi) \qquad (-\pi, 0) \qquad (\pi, 0)$$

are the same point. Thus these need to be considered once. Looking to the bulk of the rhombus,
due to s^* periodicity it suffices to integrate over one quarter (considering just one internal border)
and multiply by 4. In doing this, the origin $(0, 0)$ must be counted only once. Fig. 1.3 summarizes
this argument: if we assign to any given point $\mathbf{k} \in \mathrm{BZ}$ a weight function $w(\mathbf{k})$ defined as in figure,
in particular avoiding computations over white and gray points, we get an optimized integral over
the entire MBZ saving *circa* 75% of runtime.

1.5.2   Results of the HF algorithm at generic doping

Within this section we will ignore stability considerations. The first set of simulations was run
keeping the local repulsion fixed at a *not-so-strong* coupling value, $U/t = 4$, and letting V vary up
to a comparable value, $0 \leq V/t \leq 3$, for various fillings. The temperature is kept to a finite large
value $\beta = 100$ to avoid Fermi surface discontinuities, while lattice size is kept to a reasonably high
value $L_x = L_y = 256$ to suppress finite-size effects while keeping runtime low enough. The HF has
been set with the following parameters:

```
1  p::Int64 = 100                        # Maximum number of iterations
2  dv::Dict{String,Float64} = Dict([     # Relative tolerance on each HFP
3      "m" => 1e-4,
4      "w0" => 1e-4,
5      "wp" => 1e-4
6  ])
7  dn::Float64 = 1e-2                     # Relative tolerance on density
8  g::Float64 = 0.5                       # Mixing parameter
```

First HFP: m (magnetization).   Consider first Fig. 1.4a. As is to be expected from Eq. (1.23),
being it dependent on

$$\mathrm{Re}\{\tilde{\Delta}_{\mathbf{k}}\} = m(U + 2zV) \quad \text{with } z = 4$$

in this renormalized antiferromagnetic phase the non-local attraction acts as a magnetization boost,
essentially reproducing the same behavior of m with U for the conventional Hubbard model plotted

a | Magnetization in the UV plane.   b | Magnetization in the $V\delta$ plane.

Figure 1.5 | Heatmaps of the magnetization m in the antiferromagnetic phase in the UV plane (Fig. 1.5a) and the $V\delta$ plane (Fig. 1.5b).


a | Non-local attraction V/t de-pencence.   b | Doping $\delta = n - 0.5$ dependence.

Figure 1.6 | Plots of the parameter $w^{(\mathbf{0})}$ in the antiferromagnetic phase as a function of both the non-local attraction V/t (Fig. 1.6a) and the doping $\delta = n - 1/2$ (Fig. 1.6b), at fixed local repulsion $U/t = 4$.

in Fig. A.6. The non-local attraction also enlarges the AF phase when considering various dopings, as is seen in Fig. 1.4. The magnetized region is largely extended with respect to the low-doped segment that magnetizes at $V = 0$. These effects are not particularly interesting or surprising. However, something more interesting arises when looking to Fig. 1.5, a couple of heatmaps in UV and $V\delta$ planes obtained respectively at $\delta = 0.2$ and $U = 4.0$, with L_x halved down to 128 for computational reasons. Fig. 1.5 expresses again the boost to magnetization given by V, with a magnetized region separated by a linear boundary approximately tilted as $-1/2z$, coherently with the renormalization of $\mathrm{Re}\{\tilde{\Delta}_{\mathbf{k}}\}$. Fig. 1.5b in particular is interesting: a sort of shallow "phase boundary" appears to follow a regular sub-linear curve.

Second HFP: $w^{(\mathbf{0})}$ (hopping renormalization coefficient). Moving to the second HFP, things get interesting. Fig. 1.6 is set up as Fig. 1.4, while Fig. 1.7 as Fig. 1.5. When considering the behavior of the parameter at fixed U, thus looking to Fig. 1.6a, a series of *plateaus* later interrupted by a continuous change in derivative are present at each doping. This is clearly evident also in Fig. 1.5b, with the parameter staying constant when approaching from left the maximum situated at the position of the "phase boundary" of Fig. 1.5b. The fact that there exists a geometric region of the $V\delta$ plane where are located both the phase transition and the maximum of this parameter, which controls hopping renormalization, is particularly interesting, suggesting the possibility of finding a maximally localized system by following the path extrapolated by maximizing $w^{(\mathbf{0})}$ around the phase transition.

Interestingly enough, the highly doped region, $\delta > 0.4$, presents seemingly no dependency on

a | Magnetization   in   the UV plane.   b | Magnetization in the $V\delta$ plane.
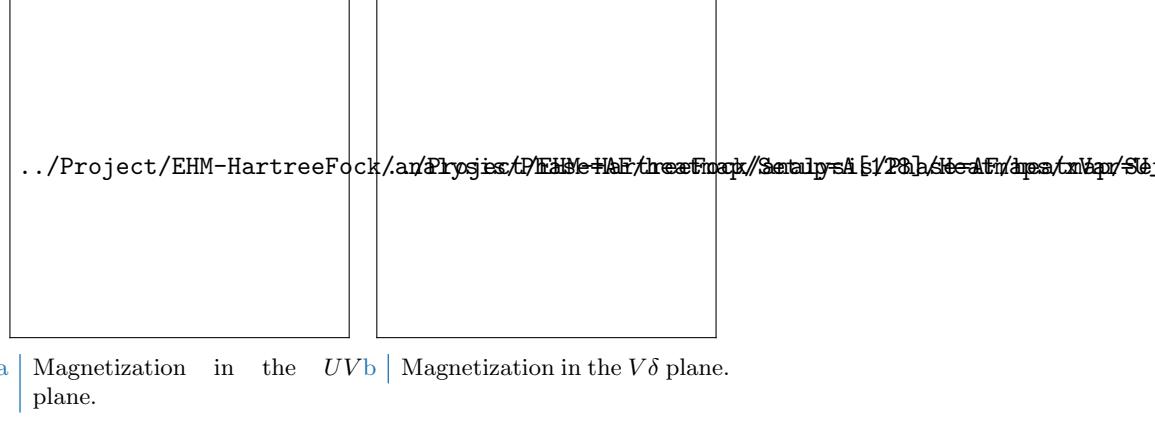
Figure 1.7 | Heatmaps of the parameter $w^{(\mathbf{0})}$ in the antiferromagnetic phase in the UV plane (Fig. 1.7a) and the $V\delta$ plane (Fig. 1.7b).

a | Effective hopping in the UV b | Effective hopping in the $V\delta$
plane.   plane.
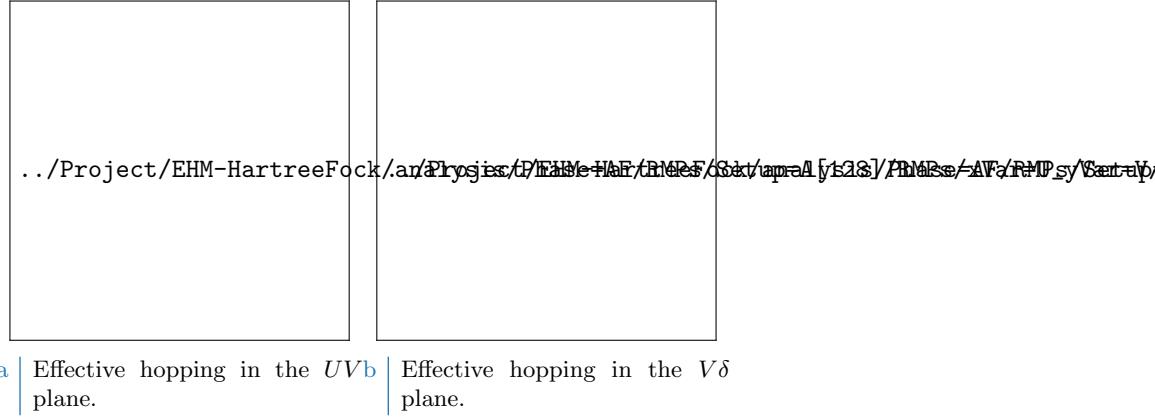
Figure 1.8 | Plots of the effective hopping $\tilde{t}$ in the antiferromagnetic phase in the UV plane (Fig. 1.8a) and the $V\delta$ plane (Fig. 1.8b).

V in Fig. 1.7b (at least for thus value of U), as is also evident from the asymptotic behavior at increasing V visible in Fig. 1.7b. Moreover, Fig. 1.5a and 1.7a appear almost reciprocal: where one parameter grows, the other is suppressed. In terms of hopping renormalization, this tells us that antiferromagnetic ordering tends to maintain t non-renormalized.

Fig. 1.8 reports in its subplots the renormalized hopping as a function of the model parameters, in the same setups as in the aforementioned heatmaps. As is depicted, the NN interaction V tends to reduce effective hopping amplitude down to a significant fraction of the starting value: t is damped of a 30% factor or so. As is evident from Fig. 1.8b, for a small local repulsion $U = 4$ the value of $\tilde{t}$ lowers as the doping grows, reaching a maximum approximately on the position of the maxima of $w^{(\mathbf{0})}$ in Fig. 1.7b, which was expected considering Eq. (1.18).

Third HFP: $w^{(\boldsymbol{\pi})}$ (imaginary gap coefficient). Unsurprisingly, the third HFP turns out to be essentially zero in all parameters space, considering also numerical fluctuations. This was expected: when deriving the MF solution to the model within AF phase, we essentially reduced it to the already known solution of Sec. A.3. The gap there was a real parameter, thus by purely renormalizing the parameters obtained within such solution there is no need for the present gap to acquire a non-zero imaginary part.

1.5.3   Role of hopping renormalization: switching off $w^{(\mathbf{0})}$

[To be continued. . .]

Chapter 2

Superconducting instability

This chapter is devoted to studying the superconducting phase of the system. The only symmetry we assume to break is the $U^c(1)$ charge symmetry, thus allowing for superconducting fluctuations. As is described thoroughly in Sec. 1.3.2, the hopping amplitude is renormalized because of the non-local attraction. The symmetry structure of the pairing mechanism determines the contributing Cooper fluctuations: for s-wave and d-wave superconductivity, only the o.s. Cooper term contributes; for p_ℓ-wave superconductivity, the s.s. term contributes as well. In the following sections, a derivation containing both Cooper terms is proposed.

[To be continued: separate singlet and triplet pairing channels, and describe them separately by the means of four-components Nambu spinors. Use selection rules to set $\Delta^{(p_\ell)} = 0$ in the singlet channel, in order to justify results obtained by a pure space-even simulation containing just the o.s. terms.]

2.1 Cooper fluctuations in the EHM

Let us start once again from the general EHM of Eq. (**??**),

$$\hat{H} = \underbrace{-t \sum_{\langle ij \rangle} \sum_\sigma \hat{c}_{i\sigma}^\dagger \hat{c}_{j\sigma}}_{\hat{H}_t} + \underbrace{U \sum_i \hat{c}_{i\uparrow}^\dagger \hat{c}_{i\downarrow}^\dagger \hat{c}_{i\downarrow} \hat{c}_{i\uparrow}}_{\hat{H}_U} \underbrace{- V \sum_{\langle ij \rangle} \sum_{\sigma\sigma'} \hat{c}_{i\sigma}^\dagger \hat{c}_{j\sigma'}^\dagger \hat{c}_{j\sigma'} \hat{c}_{i\sigma}}_{\hat{H}_V}$$

As is discussed in Sec. **??**, when applying Wick's theorem the resulting terms break the natural symmetries of the model. The superconducting symmetry we study breaks just the $U^c(1)$ charge conservation. Now, when dealing with superconducting Cooper pairing we need to account also for the spatial structure of the Cooper pair itself. Consider the generic Cooper fluctuation

$$\langle \hat{c}_{i\sigma}^\dagger \hat{c}_{j\sigma'}^\dagger \rangle \quad \text{with } i, j \text{ NN}$$

From basic Quantum Mechanics we know the summation rules of the spin algebra $\mathfrak{su}(2)$,

$$\frac{1}{2} \otimes \frac{1}{2} = 0 \oplus 1$$

The two pairing channels are, at this level, the singlet channel associated to total spin 0 and the triplet channel associated to total spin 1. If we impose a specific spatial symmetry on the hamiltonian the ground state wavefunction will follow naturally, and the pairing channel will be the one providing a total anti-symmetry to the full wavefunction. This gives a selection rule over the relevant pairings: if we work with space symmetric structures – say, s^*-wave or d-wave – the pairing will happen in singlet channel, allowing us to eliminate the triplet pairing. This concept is summarized in Tab. 2.1.

[Add: Cooper pairing considerations in the pure Hubbard model.]

2.2 Cooper fluctuations in the opposite-spin sector

This section deals with Cooper fluctuations induced by the o.s. part of the non-local hamiltonian –referring to the notation of Eq. (**??**)– somewhat the simplest form of Cooper pairing. This sector

Spatial structure	Pairing channel	Relevant pairing
Symmetric wave function	Singlet pairing	Just $\langle \hat{c}_{i\sigma}^\dagger \hat{c}_{j\bar\sigma}^\dagger \rangle$
Anti-symmetric wave function	Triplet pairing	Both $\langle \hat{c}_{i\sigma}^\dagger \hat{c}_{j\bar\sigma}^\dagger \rangle$ and $\langle \hat{c}_{i\sigma}^\dagger \hat{c}_{j\sigma}^\dagger \rangle$

Table 2.1 | Relation of the Cooper pairing channell with the wavefunction spatial symmetry (intended as the inversion $(x,y) \to (-x,-y)$).

contributes both to singlet pairing and triplet pairing. Considering Cooper fluctuations in the singlet channel, we need to break $U^c(1)$ symmetry imposing space inversion symmetry, while for the triplet anti-symmetry is required. Let us now break down the MFT discussion for the local and non-local interactions.

Local interaction U. Consider first the local part,

$$\hat{H}_U = U \sum_{i \in \mathcal{S}} \hat{n}_{i\uparrow} \hat{n}_{i\downarrow} \simeq U \sum_{i \in \mathcal{S}} \left[\langle \hat{c}_{i\uparrow}^\dagger \hat{c}_{i\downarrow}^\dagger \rangle \hat{c}_{i\downarrow} \hat{c}_{i\uparrow} + \hat{c}_{i\uparrow}^\dagger \hat{c}_{i\downarrow}^\dagger \langle \hat{c}_{i\downarrow} \hat{c}_{i\uparrow} \rangle \right]$$

and use the result of Eq. (**??**),

$$\hat{H}_U \simeq \frac{U}{L_x L_y} \sum_{\mathbf{K},\mathbf{k},\mathbf{k}'} \left[\langle \hat{c}_{\mathbf{K}+\mathbf{k}\uparrow}^\dagger \hat{c}_{\mathbf{K}-\mathbf{k}\downarrow}^\dagger \rangle \hat{c}_{\mathbf{K}-\mathbf{k}'\downarrow} \hat{c}_{\mathbf{K}+\mathbf{k}'\uparrow} + \hat{c}_{\mathbf{K}+\mathbf{k}\uparrow}^\dagger \hat{c}_{\mathbf{K}-\mathbf{k}\downarrow}^\dagger \langle \hat{c}_{\mathbf{K}-\mathbf{k}'\downarrow} \hat{c}_{\mathbf{K}+\mathbf{k}'\uparrow} \rangle \right]$$

We are not breaking translational invariance, thus only Cooper fluctuations with net zero total momentum are allowed. This means only $\mathbf{K} = \mathbf{0}$ contributes. Define the pairing operator

$$\hat{\phi}_{\mathbf{k}} \equiv \hat{c}_{-\mathbf{k}\downarrow} \hat{c}_{\mathbf{k}\uparrow} \qquad \hat{\phi}_{\mathbf{k}}^\dagger \equiv \hat{c}_{\mathbf{k}\uparrow}^\dagger \hat{c}_{-\mathbf{k}\downarrow}^\dagger$$

Then the non local repulsion reduces to the ordinary BCS-like interaction,

$$\hat{H}_U \simeq \sum_{\mathbf{k}} \left[\mathcal{U}_{\mathbf{k}} \hat{\phi}_{\mathbf{k}} + \mathcal{U}_{\mathbf{k}}^* \hat{\phi}_{\mathbf{k}}^\dagger \right] \tag{2.1}$$

where the MFT parameter $\mathcal{U}_{\mathbf{k}}$ must satisfy the self-consistency equation

$$\mathcal{U}_{\mathbf{k}} \equiv \frac{U}{L_x L_y} \sum_{\mathbf{k}} \langle \hat{\phi}_{\mathbf{k}}^\dagger \rangle \tag{2.2}$$

Note that $\mathcal{U}_{\mathbf{k}}$ is actually momentum independent. This is due to the fact that the repulsion is completely localized.

Non-local interaction V. The non-local attraction in the opposite-spin sector of $\hat{H}_V$ is given by

$$\hat{H}_V^{(\text{o.s.})} = -V \sum_{\langle ij \rangle} \sum_{\sigma} \hat{n}_{i\sigma} \hat{n}_{j\bar\sigma}$$

which, using Eq. (**??**) and performing Wick's contractions, reduces to:

$$\hat{H}_V^{(\text{o.s.})} = -V \sum_{i \in \mathcal{S}} \sum_{\ell=x,y} \sum_{\delta=\pm\delta_\ell} \hat{n}_{i\uparrow} \hat{n}_{i+\delta\downarrow}$$

$$\simeq -V \sum_{i \in \mathcal{S}} \sum_{\ell=x,y} \sum_{\delta=\pm\delta_\ell} \left[\langle \hat{c}_{i\uparrow}^\dagger \hat{c}_{i+\delta\downarrow}^\dagger \rangle \hat{c}_{i+\delta\downarrow} \hat{c}_{i\uparrow} + \hat{c}_{i\uparrow}^\dagger \hat{c}_{i+\delta\downarrow}^\dagger \langle \hat{c}_{i+\delta\downarrow} \hat{c}_{i\uparrow} \rangle \right]$$

Using Eq. (**??**) we can move to reciprocal space,

$$\hat{H}_V^{(\text{o.s.})} \simeq -\frac{V}{L_x L_y} \sum_{\mathbf{K},\mathbf{k},\mathbf{k}'} \left[\cos(\delta k_x) + \cos(\delta k_y) \right]$$

$$\times \left[\langle \hat{c}_{\mathbf{K}+\mathbf{k}\uparrow}^\dagger \hat{c}_{\mathbf{K}-\mathbf{k}\downarrow}^\dagger \rangle \hat{c}_{\mathbf{K}-\mathbf{k}'\downarrow} \hat{c}_{\mathbf{K}+\mathbf{k}'\uparrow} + \hat{c}_{\mathbf{K}+\mathbf{k}\uparrow}^\dagger \hat{c}_{\mathbf{K}-\mathbf{k}\downarrow}^\dagger \langle \hat{c}_{\mathbf{K}-\mathbf{k}'\downarrow} \hat{c}_{\mathbf{K}+\mathbf{k}'\uparrow} \rangle \right]$$

Identical considerations as above hold, and just the $\mathbf{K} = \mathbf{0}$ term contributes. We have finally

$$\hat{H}_V^{(\text{o.s.})} \simeq -\sum_{\mathbf{k},\mathbf{k}'} V_{\mathbf{k}\mathbf{k}'} \left[\langle \hat{\phi}_{\mathbf{k}}^\dagger \rangle \hat{\phi}_{\mathbf{k}'} + \langle \hat{\phi}_{\mathbf{k}} \rangle \hat{\phi}_{\mathbf{k}'}^\dagger \right]$$

where the two-body potential was defined

$$V_{\mathbf{k}\mathbf{k}'} = \frac{V}{L_x L_y} \left[\cos\left(\delta k_x\right) + \cos\left(\delta k_y\right) \right]$$

Making use of the decomposition of Eq. (**??**), the two-body potential becomes

$$\begin{aligned} V_{\mathbf{k}\mathbf{k}'} &= \frac{V}{2L_x L_y} \sum_\gamma \varphi_{\mathbf{k}}^{(\gamma)} \varphi_{\mathbf{k}'}^{(\gamma)*} \\ &= \sum_\gamma V^{(\gamma)} \varphi_{\mathbf{k}}^{(\gamma)} \varphi_{\mathbf{k}'}^{(\gamma)*} \end{aligned}$$

being $\gamma \in \{s^*, p_x, p_y, d_{x^2-y^2}\}$ and $\varphi_{\mathbf{k}}^{(\gamma)}$ the reciprocal-space expressions for the form factors of Tab. **??**, listed explicitly in Tab. **??**, and $V_{\mathbf{k}\mathbf{k}'}^{(\gamma)}$ the symmetry-resolved components of the non-local attraction. Then the two-body potential has been decomposed in its planar symmetry components, each of which will naturally couple only to identically structured parameters in the full hamiltonian.

Define now the non-local gap function

$$\mathcal{V}_{\mathbf{k}} \equiv \sum_{\mathbf{k}'} V_{\mathbf{k}\mathbf{k}'} \langle \hat{\phi}_{\mathbf{k}'}^\dagger \rangle \tag{2.3}$$

one gets immediately

$$\hat{H}_V \simeq -\sum_{\mathbf{k}} \left[\mathcal{V}_{\mathbf{k}} \hat{\phi}_{\mathbf{k}} + \mathcal{V}_{\mathbf{k}}^* \hat{\phi}_{\mathbf{k}}^\dagger \right] \tag{2.4}$$

To assume symmetry is broken in a specific symmetry channel γ means precisely to assume $\langle \hat{\phi}_{\mathbf{k}} \rangle \propto \varphi_{\mathbf{k}}^{(\gamma)}$. Of course, in Eq. (2.3) only the γ component of the potential survives, implying the gap function acquires the same symmetry,

$$\mathcal{V}_{\mathbf{k}} \propto \sum_{\mathbf{k}'} \varphi_{\mathbf{k}}^{(\gamma)} \varphi_{\mathbf{k}'}^{(\gamma)*} \varphi_{\mathbf{k}'}^{(\gamma)} \propto \varphi_{\mathbf{k}}^{(\gamma)}$$

where orthonormality of the $\varphi_{\mathbf{k}}^{(\gamma)}$ functions of Tab. **??** was used. Thus, assuming to have superconductivity in a given sector γ, the self consistency equation reads

$$\forall \gamma \in \{s^*, p_x, p_y, d_{x^2-y^2}\} \qquad \mathcal{V}_{\mathbf{k}}\big|_\gamma \equiv \frac{V}{2L_x L_y} \sum_{\mathbf{k}} \varphi_{\mathbf{k}}^{(\gamma)} \langle \hat{\phi}_{\mathbf{k}}^\dagger \rangle \tag{2.5}$$

Now we merge the two interaction in a single gap function.

2.2.1 Full gap function and self-consistency equations

Define the full gap function as the sum of both contributions,

$$\Delta_{\mathbf{k}} \equiv \mathcal{V}_{\mathbf{k}} - \mathcal{U}_{\mathbf{k}} \tag{2.6}$$

The full self-consistency equation is given by the simple combination of Eqns. (2.2) and (2.5),

$$\Delta_{\mathbf{k}} \equiv \sum_{\mathbf{k}'} \left[V^{(s)} + V_{\mathbf{k}\mathbf{k}'} \right] \langle \hat{\phi}_{\mathbf{k}'}^\dagger \rangle \quad \text{with} \quad V^{(s)} = -\frac{U}{2L_x L_y} \tag{2.7}$$

The gap function decomposes in symmetry channels as well,

$$\Delta_{\mathbf{k}} = \sum_\gamma \Delta^{(\gamma)} \varphi_{\mathbf{k}}^{(\gamma)}$$

Structure	Self-consistency equation	Graph
s-wave	$\Delta^{(s)} = -\dfrac{U}{2L_xL_y} \displaystyle\sum_{\mathbf{k}} \langle \hat{\phi}_{\mathbf{k}}^{\dagger} \rangle$	Fig. **??**
Extended s-wave	$\Delta^{(s^*)} = \dfrac{V}{L_xL_y} \displaystyle\sum_{\mathbf{k}} (c_x + c_y)\langle \hat{\phi}_{\mathbf{k}}^{\dagger} \rangle$	Fig. **??**
p_x-wave	$\Delta^{(p_x)} = -i\sqrt{2}\dfrac{V}{L_xL_y} \displaystyle\sum_{\mathbf{k}} s_x\langle \hat{\phi}_{\mathbf{k}}^{\dagger} \rangle$	Fig. **??**
p_y-wave	$\Delta^{(p_y)} = -i\sqrt{2}\dfrac{V}{L_xL_y} \displaystyle\sum_{\mathbf{k}} s_y\langle \hat{\phi}_{\mathbf{k}}^{\dagger} \rangle$	Fig. **??**
$d_{x^2-y^2}$-wave	$\Delta^{(d)} = \dfrac{V}{L_xL_y} \displaystyle\sum_{\mathbf{k}} (c_x - c_y)\langle \hat{\phi}_{\mathbf{k}}^{\dagger} \rangle$	Fig. **??**

Table 2.2 | Symmetry resolved self-consistency equations for the MFT parameters $\Delta^{(\gamma)}$, based on Eq. (2.7) and (2.8). By computing $\langle \hat{\phi}_{\mathbf{k}}^{\dagger} \rangle$, it is possible to reconstruct the various components of the gap function.

If SC arises in a specific symmetry channel, $\Delta_{\mathbf{k}}$ will show the same symmetry. It follows, due to orthonormality and using Eq. (2.7),

$$
\begin{aligned}
\Delta^{(\gamma)} &= \frac{1}{L_xL_y} \sum_{\mathbf{k}} \varphi_{\mathbf{k}}^{(\gamma)*} \Delta_{\mathbf{k}} \\
&= \frac{1}{L_xL_y} \sum_{\mathbf{k}} \varphi_{\mathbf{k}}^{(\gamma)*} \sum_{\mathbf{k}'} \left[V^{(s)} + V_{\mathbf{kk}'} \right] \langle \hat{\phi}_{\mathbf{k}'}^{\dagger} \rangle \\
&= \frac{1}{L_xL_y} \sum_{\mathbf{k}} \varphi_{\mathbf{k}}^{(\gamma)*} \sum_{\mathbf{k}'\gamma'} V^{(\gamma')} \varphi_{\mathbf{k}}^{(\gamma')} \varphi_{\mathbf{k}'}^{(\gamma')*} \langle \hat{\phi}_{\mathbf{k}'}^{\dagger} \rangle \\
&= V^{(\gamma)} \sum_{\mathbf{k}} \varphi_{\mathbf{k}}^{(\gamma)*} \langle \hat{\phi}_{\mathbf{k}}^{\dagger} \rangle
\end{aligned}
\tag{2.8}
$$

This result provides a set of self-consistency equations for each symmetry channel, listed in Tab. 2.2. Notice that to reconstruct self-consistently the full s-wave phase transition, the actual gap function is given by

$$
\Delta^{(s)} + \Delta^{(s^*)}(c_x + c_y)
$$

The s-wave transition is the only one equipped of both the local and the non-local parts.

2.2.2   Non-local bands renormalization in the same-spin sector

In the context of antiferromagnetism (Sec. 1.3.2) we discussed the role of the non-local interaction $\hat{H}_V$ as a source of bands effective renormalization. One of the most interesting results was the on of Eq. (1.18), with the hopping parameter being rigidly shifted. In the present context, we aim to treat the non-local part similarly by using immediately the aforementioned results. Start from Eq. (1.13),

$$
\begin{aligned}
V \sum_{\langle ij \rangle} \sum_{\sigma} & \left[\langle \hat{c}_{i\sigma}^{\dagger} \hat{c}_{j\sigma} \rangle \hat{c}_{j\sigma}^{\dagger} \hat{c}_{i\sigma} + \text{h.c.} \right] \\
&= \frac{2V}{L_xL_y} \sum_{\mathbf{K},\mathbf{k},\mathbf{k}'} \sum_{\sigma} \left[\cos(\delta k_x) + \cos(\delta k_y) \right] \langle \hat{c}_{\mathbf{K}+\mathbf{k}\sigma}^{\dagger} \hat{c}_{\mathbf{K}-\mathbf{k}'\sigma} \rangle \hat{c}_{\mathbf{K}-\mathbf{k}\sigma}^{\dagger} \hat{c}_{\mathbf{K}+\mathbf{k}'\sigma}
\end{aligned}
$$

For the BCS ground state, it is immediate to see the only relevant contribution comes from

$$
\mathbf{k} = -\mathbf{k}'
$$

which gives the diagonal part of Eq. (1.14). We are then left with (half) the result of Eq. (1.15)

$$V \sum_{\langle ij \rangle} \sum_{\sigma} \left[\langle \hat{c}_{i\sigma}^{\dagger} \hat{c}_{j\sigma} \rangle \hat{c}_{j\sigma}^{\dagger} \hat{c}_{i\sigma} + \text{h.c.} \right] = \frac{2V}{L_x L_y} \sum_{\mathbf{q},\mathbf{q}'} \sum_{\sigma} \left[\cos\left(\delta q_x\right) + \cos\left(\delta q_y\right) \right] \langle \hat{c}_{\mathbf{q}\sigma}^{\dagger} \hat{c}_{\mathbf{q}\sigma} \rangle \hat{c}_{\mathbf{q}'\sigma}^{\dagger} \hat{c}_{\mathbf{q}'\sigma} \quad (2.9)$$

Recall Eq. (**??**): the structure term decomposes in harmonic waves, and this feature is particularly handy in order to decouple the $\mathbf{q}$ and $\mathbf{q}'$ parts, as we later do.

2.3 Superconducting solution in the Nambu formalism

As a first approach to anisotropic SC in the Hubbard model, let us discuss the superconducting solutions in the simple scenario where crystal translational invariance is preserved and thus the system can be treated by the means of common BCS. As will be discussed, the non-local attraction acts as a source of SC in all symmetry sectors.

Define the Nambu spinor[1] as in BCS

$$\hat{\Psi}_{\mathbf{k}} \equiv \begin{bmatrix} \hat{c}_{\mathbf{k}\uparrow} \\ \hat{c}_{-\mathbf{k}\downarrow}^{\dagger} \end{bmatrix}$$

Evidently,

$$\phi_{\mathbf{k}} = \hat{\Psi}_{\mathbf{k}}^{\dagger} \begin{bmatrix} 0 & 1 \\ 0 & 0 \end{bmatrix} \hat{\Psi}_{\mathbf{k}} \qquad \phi_{\mathbf{k}}^{\dagger} = \hat{\Psi}_{\mathbf{k}}^{\dagger} \begin{bmatrix} 0 & 0 \\ 1 & 0 \end{bmatrix} \hat{\Psi}_{\mathbf{k}} \quad (2.10)$$

The full hamiltonian is then given by:

$$\hat{H} = \sum_{\mathbf{k}} \hat{\Psi}_{\mathbf{k}} h_{\mathbf{k}} \hat{\Psi}_{\mathbf{k}} \qquad h_{\mathbf{k}} \equiv \begin{bmatrix} \epsilon_{\mathbf{k}} & -\Delta_{\mathbf{k}}^{*} \\ -\Delta_{\mathbf{k}} & -\epsilon_{\mathbf{k}} \end{bmatrix} \quad (2.11)$$

Next step is to perform the well-known Bogoliubov transform and reduce all the problem down to a simple ensemble of quantum pseudospins.

2.3.1 Bogoliubov transform and pseudospins picture

Let τ^{α} for $\alpha = x, y, z$ be the Pauli matrices. Define the pseudospin operator:

$$\hat{s}_{\mathbf{k}}^{\alpha} \equiv \hat{\Psi}_{\mathbf{k}}^{\dagger} \tau^{\alpha} \hat{\Psi}_{\mathbf{k}} \quad \text{for} \quad \alpha = x, y, z$$

As can be shown easily, these operators realize spin-1/2 algebra. $\hat{H}$ represents an ensemble of $L_x L_y$ independent spins subject to pseudo-magnetic fields. Note that, differently form App. **??** where the chemical potential is inserted later (because in Nambu formalism it accounts for a diagonal term) here the chemical potential is part of the z component of the pseudo-magnetic field, since

$$
\begin{aligned}
\hat{n}_{\mathbf{k}\uparrow} + \hat{n}_{-\mathbf{k}\downarrow} &= \hat{c}_{\mathbf{k}\uparrow}^{\dagger} \hat{c}_{\mathbf{k}\uparrow} + \hat{c}_{-\mathbf{k}\downarrow}^{\dagger} \hat{c}_{-\mathbf{k}\downarrow} \\
&= \hat{c}_{\mathbf{k}\uparrow}^{\dagger} \hat{c}_{\mathbf{k}\uparrow} - \hat{c}_{-\mathbf{k}\downarrow} \hat{c}_{-\mathbf{k}\downarrow}^{\dagger} + \mathbb{I} \\
&= \hat{\Psi}_{\mathbf{k}}^{\dagger} \tau^{z} \hat{\Psi}_{\mathbf{k}} + \mathbb{I}
\end{aligned}
\quad (2.12)
$$

and then it follows

$$
\begin{aligned}
-\mu \hat{N} &= -\mu \sum_{\mathbf{k} \in \text{BZ}} \left[\hat{n}_{\mathbf{k}\uparrow} + \hat{n}_{-\mathbf{k}\downarrow} \right] \\
&= -\mu \sum_{\mathbf{k} \in \text{BZ}} \hat{\Psi}_{\mathbf{k}}^{\dagger} \tau^{z} \hat{\Psi}_{\mathbf{k}} - \mu L_x L_y
\end{aligned}
$$

Then, adding a term $-\mu \hat{N}$ to $\hat{H}$, apart from an irrelevant total energy increase, changes the pseudo-field whose explicit form becomes

$$\mathbf{b}_{\mathbf{k}} \equiv \begin{bmatrix} -\operatorname{Re}\{\Delta_{\mathbf{k}}\} \\ -\operatorname{Im}\{\Delta_{\mathbf{k}}\} \\ \epsilon_{\mathbf{k}} - \mu \end{bmatrix} \quad (2.13)$$

---

[1]Notice that the spinor is here differently defined with respect to App. A, where because of the HF prevalence in mean-field decoupling the spinor components were homogeneously fermions creations or destructions.

This hamiltonian behaves as an ensemble of spins in local magnetic fields precisely as in Eq. (A.6),

$$\hat{H} - \mu\hat{N} = \sum_{\mathbf{k}\in\mathrm{BZ}} \mathbf{b_k} \cdot \hat{\mathbf{s}}_\mathbf{k} \quad \text{where} \quad \hat{\mathbf{s}}_\mathbf{k} = \begin{bmatrix} \hat{s}^x_\mathbf{k} \\ \hat{s}^y_\mathbf{k} \\ \hat{s}^z_\mathbf{k} \end{bmatrix} \tag{2.14}$$

Proceed as in App. **??** and diagonalize via a rotation,

$$d_\mathbf{k} \equiv \begin{bmatrix} -E_\mathbf{k} & \\ & E_\mathbf{k} \end{bmatrix} \quad \text{being} \quad E_\mathbf{k} \equiv \sqrt{\xi_\mathbf{k}^2 + |\Delta_\mathbf{k}|^2}$$

and $\xi_\mathbf{k} \equiv \epsilon_\mathbf{k} - \mu$. Given the pseudoangles

$$\tan(2\theta_\mathbf{k}) \equiv \frac{|\Delta_\mathbf{k}|}{\xi_\mathbf{k}} \qquad \tan(2\zeta_\mathbf{k}) \equiv \frac{\mathrm{Im}\{\Delta_\mathbf{k}\}}{\mathrm{Re}\{\Delta_\mathbf{k}\}}$$

the general diagonalizer will be an orthogonal rotation matrix

$$\begin{aligned} W_\mathbf{k} &= e^{i\left(\theta_\mathbf{k} - \frac{\pi}{2}\right)\tau^y} e^{i\zeta_\mathbf{k}\tau^z} \\ &= \begin{bmatrix} -\sin\theta_\mathbf{k} & -\cos\theta_\mathbf{k} \\ \cos\theta_\mathbf{k} & -\sin\theta_\mathbf{k} \end{bmatrix} \begin{bmatrix} e^{i\zeta_\mathbf{k}} & \\ & e^{-i\zeta_\mathbf{k}} \end{bmatrix} \\ &= \begin{bmatrix} -\sin\theta_\mathbf{k} e^{i\zeta_\mathbf{k}} & -\cos\theta_\mathbf{k} e^{-i\zeta_\mathbf{k}} \\ \cos\theta_\mathbf{k} e^{i\zeta_\mathbf{k}} & -\sin\theta_\mathbf{k} e^{-i\zeta_\mathbf{k}} \end{bmatrix} \end{aligned} \tag{2.15}$$

given by a rotation of angle $\zeta_\mathbf{k}$ around the z axis, to align the x axis with the field projection onto the xy plane, followed by a rotation around the y axis to anti-align with the pseudo-field.

2.3.2   BCS ground state properties

The MFT-BCS solution is given by a degenerate Fermi gas at ground state, whose quasi-particles occupy two bands $\pm E_\mathbf{k}$ and their fermionic operators are given by

$$\hat{\gamma}^{(-)}_\mathbf{k} \equiv \left[W_\mathbf{k}\hat{\Psi}_\mathbf{k} \right]_1 \qquad \hat{\gamma}^{(+)}_\mathbf{k} \equiv \left[W_\mathbf{k}\hat{\Psi}_\mathbf{k} \right]_2$$

The diagonalization operators are given by

$$\hat{\Gamma}_\mathbf{k} \equiv W_\mathbf{k}\hat{\Psi}_\mathbf{k} \quad \text{where} \quad \hat{\Gamma}_\mathbf{k} = \begin{bmatrix} \hat{\gamma}^{(-)}_\mathbf{k} \\ \hat{\gamma}^{(+)}_\mathbf{k} \end{bmatrix}$$

Using Eq. (A.15),

$$\left\langle [\hat{\Psi}^\dagger_\mathbf{k}]_i [\hat{\Psi}_\mathbf{k}]_j \right\rangle = [W_\mathbf{k}]_{1i}[W^\dagger_\mathbf{k}]_{j1} f\left(-E_\mathbf{k}; \beta, 0\right) + [W_\mathbf{k}]_{2i}[W^\dagger_\mathbf{k}]_{j2} f\left(E_\mathbf{k}; \beta, 0\right)$$

where in the Fermi-Dirac function chemical potential was set to zero, because it already was included in the diagonalized hamiltonian. Recalling Eq. (**??**), it follows for $i = 1$, $j = 2$

$$\langle \hat{\phi}^\dagger_\mathbf{k} \rangle = [W_\mathbf{k}]_{11}[W^\dagger_\mathbf{k}]_{21} f\left(-E_\mathbf{k}; \beta, 0\right) + [W_\mathbf{k}]_{21}[W^\dagger_\mathbf{k}]_{22} f\left(E_\mathbf{k}; \beta, 0\right) \tag{2.16}$$

$$= \frac{1}{2}\sin\left(2\theta_\mathbf{k}\right) e^{i2\zeta_\mathbf{k}} \tanh\left(\frac{\beta E_\mathbf{k}}{2}\right) \tag{2.17}$$

The last passage has been obtained by computing the matrix element from the explicit form of $W_\mathbf{k}$ of Eq. (2.15) and by the simple relation

$$\frac{1}{e^{-x}+1} - \frac{1}{e^x+1} = \frac{e^x - 1}{e^x + 1}$$

$$= \tanh\left(\frac{x}{2}\right)$$

Similarly, for $i = 1$, $j = 1$

$$\langle \hat{c}^{\dagger}_{\mathbf{k}\uparrow} \hat{c}_{\mathbf{k}\uparrow} \rangle = [W_{\mathbf{k}}]_{11}[W^{\dagger}_{\mathbf{k}}]_{11} f(-E_{\mathbf{k}}; \beta, 0) + [W_{\mathbf{k}}]_{21}[W^{\dagger}_{\mathbf{k}}]_{12} f(E_{\mathbf{k}}; \beta, 0) \tag{2.18}$$
$$= \sin^2 \theta_{\mathbf{k}} f(-E_{\mathbf{k}}; \beta, 0) + \cos^2 \theta_{\mathbf{k}} f(E_{\mathbf{k}}; \beta, 0)$$
$$= \sin^2 \theta_{\mathbf{k}} \tanh\left(\frac{\beta E_{\mathbf{k}}}{2}\right) + f(E_{\mathbf{k}}; \beta, 0) \tag{2.19}$$

and for $i = 2$, $j = 2$

$$\langle \hat{c}_{-\mathbf{k}\downarrow} \hat{c}^{\dagger}_{-\mathbf{k}\downarrow} \rangle = [W_{\mathbf{k}}]_{12}[W^{\dagger}_{\mathbf{k}}]_{21} f(-E_{\mathbf{k}}; \beta, 0) + [W_{\mathbf{k}}]_{22}[W^{\dagger}_{\mathbf{k}}]_{22} f(E_{\mathbf{k}}; \beta, 0) \tag{2.20}$$
$$= \cos^2 \theta_{\mathbf{k}} f(-E_{\mathbf{k}}; \beta, 0) + \sin^2 \theta_{\mathbf{k}} f(E_{\mathbf{k}}; \beta, 0)$$
$$= \cos^2 \theta_{\mathbf{k}} \tanh\left(\frac{\beta E_{\mathbf{k}}}{2}\right) + f(E_{\mathbf{k}}; \beta, 0) \tag{2.21}$$

Gap function. Eqns. (2.16), (2.17) give us both the algorithmic formula (first row) and its theoretical counterpart (second row) to compute the order parameters in the HF approach at each point in k-space (k_x, k_y). We can finally derive the BCS self-consistency equation

$$\Delta_{\mathbf{k}} \equiv \frac{1}{2} \sum_{\mathbf{k}'} \left[V^{(s)} + V_{\mathbf{k}\mathbf{k}'} \right] \frac{|\Delta_{\mathbf{k}'}|}{\sqrt{\xi^2_{\mathbf{k}'} + |\Delta_{\mathbf{k}'}|^2}} \exp\left\{ i \arctan\left(\frac{\text{Im}\{\Delta_{\mathbf{k}'}\}}{\text{Re}\{\Delta_{\mathbf{k}'}\}} \right) \right\} \tanh\left(\frac{\beta}{2} \sqrt{\xi^2_{\mathbf{k}'} + |\Delta_{\mathbf{k}'}|^2} \right)$$
$$= \frac{1}{2} \sum_{\mathbf{k}'} \left[V^{(s)} + V_{\mathbf{k}\mathbf{k}'} \right] \frac{\Delta_{\mathbf{k}'}}{\sqrt{\xi^2_{\mathbf{k}'} + |\Delta_{\mathbf{k}'}|^2}} \tanh\left(\frac{\beta}{2} \sqrt{\xi^2_{\mathbf{k}'} + |\Delta_{\mathbf{k}'}|^2} \right) \tag{2.22}$$

The whole point of the HF algorithm is to find an iterative solution for each symmetry channel, using the self-consistency equation projection of Tab. 2.2.

System density. The z component of the spin operators is related to density: using Eq. (A.15),

$$\langle \hat{\Psi}^{\dagger}_{\mathbf{k}} \tau^z \hat{\Psi}_{\mathbf{k}} \rangle = \left\langle [\hat{\Psi}^{\dagger}_{\mathbf{k}}]_1 [\hat{\Psi}_{\mathbf{k}}]_1 \right\rangle - \left\langle [\hat{\Psi}^{\dagger}_{\mathbf{k}}]_2 [\hat{\Psi}_{\mathbf{k}}]_2 \right\rangle$$

Proceed as previously, and from Eq. (2.12),

$$\langle \hat{n}_{\mathbf{k}\uparrow} \rangle + \langle \hat{n}_{-\mathbf{k}\downarrow} \rangle = 1 + \langle \hat{\Psi}^{\dagger}_{\mathbf{k}} \tau^z \hat{\Psi}_{\mathbf{k}} \rangle$$
$$= 1 + \left(|[W_{\mathbf{k}}]_{11}|^2 - |[W_{\mathbf{k}}]_{12}|^2 \right) f(-E_{\mathbf{k}}; \beta, 0)$$
$$+ \left(|[W_{\mathbf{k}}]_{21}|^2 - |[W_{\mathbf{k}}]_{22}|^2 \right) f(E_{\mathbf{k}}; \beta, 0) \tag{2.23}$$
$$= 1 - \cos(2\theta_{\mathbf{k}}) \tanh\left(\frac{\beta E_{\mathbf{k}}}{2} \right) \tag{2.24}$$

coherently with Eqns. (2.19) and (2.21). The expectation value for the density is needed in order to extract the optimal chemical potential μ for the target density we aim to simulate at the given parametrization. This is numerically obtained by using Eq. (2.23) directly on the diagonalization matrix of $h_{\mathbf{k}}$.

Ground state at zero temperature. Let $\beta \to +\infty$. The basic BCS grond state is well known and identical in the present discussion. It is easily obtained by considering the zero-temperature ground state of the pseudospin hamiltonian of Eq. (2.11),

$$|\text{BCS}\rangle = \bigotimes_{\mathbf{k}} |2\theta_{\mathbf{k}}\rangle \tag{2.25}$$

where $|2\theta_{\mathbf{k}}\rangle$ is the up-state for the $\mathbf{k}$-th rotated pseudospin operator $\hat{\Gamma}^{\dagger}_{\mathbf{k}} \tau^z \hat{\Gamma}_{\mathbf{k}}$ (consider a diagram analogous to Fig. 1.1). Said state can be expressed, making use of the non-rotated pseudospin operator $\hat{\Psi}^{\dagger}_{\mathbf{k}} \tau^z \hat{\Psi}_{\mathbf{k}}$ up and down states

$$\text{up: } |\Uparrow_{\mathbf{k}}\rangle \qquad \text{down: } |\Downarrow_{\mathbf{k}}\rangle$$

by the means of a simple Bloch's representation [Redo this computation...],

$$|2\theta_{\mathbf{k}}\rangle = \cos\theta_{\mathbf{k}}|\Downarrow_{\mathbf{k}}\rangle - \sin\theta_{\mathbf{k}}|\Uparrow_{\mathbf{k}}\rangle \tag{2.26}$$

Due to Eq. (2.12) it holds

$$\left[\hat{\Psi}_{\mathbf{k}}^{\dagger}\tau^{z}\hat{\Psi}_{\mathbf{k}} + \mathbb{I}\right]|\Uparrow_{\mathbf{k}}\rangle = 2|\Uparrow_{\mathbf{k}}\rangle \quad\implies\quad |\Uparrow_{\mathbf{k}}\rangle = -\hat{\phi}_{\mathbf{k}}^{\dagger}|\Omega_{\mathbf{k}}\rangle$$

$$\left[\hat{\Psi}_{\mathbf{k}}^{\dagger}\tau^{z}\hat{\Psi}_{\mathbf{k}} + \mathbb{I}\right]|\Downarrow_{\mathbf{k}}\rangle = 0 \quad\implies\quad |\Downarrow_{\mathbf{k}}\rangle = |\Omega_{\mathbf{k}}\rangle$$

being $|\Omega_{\mathbf{k}}\rangle$ the local electron vacuum,

$$|\Omega\rangle = \bigotimes_{\mathbf{k}}|\Omega_{\mathbf{k}}\rangle$$

Taking Eq. (2.25), combined with Eq. (2.26), we get

$$\begin{aligned}|\mathrm{BCS}\rangle &= \bigotimes_{\mathbf{k}}\left[\cos\theta_{\mathbf{k}}|\Downarrow_{\mathbf{k}}\rangle - \sin\theta_{\mathbf{k}}|\Uparrow_{\mathbf{k}}\rangle\right]\\ &= \bigotimes_{\mathbf{k}}\left[\cos\theta_{\mathbf{k}} + \sin\theta_{\mathbf{k}}\hat{\phi}_{\mathbf{k}}^{\dagger}\right]|\Omega_{\mathbf{k}}\rangle\end{aligned} \tag{2.27}$$

which is the well-known coherent BCS state.

2.3.3   Renormalization of the bare bands

We now deal with the renormalization of bare bands anticipated in Sec. 2.2.2. Taking together Eqns. (2.9), (2.16) and (2.17) we get:

$$\begin{aligned}V\sum_{\langle ij\rangle}\sum_{\sigma}&\left[\langle\hat{c}_{i\sigma}^{\dagger}\hat{c}_{j\sigma}\rangle\hat{c}_{j\sigma}^{\dagger}\hat{c}_{i\sigma} + \mathrm{h.c.}\right] = \frac{2V}{L_x L_y}\sum_{\mathbf{q},\mathbf{q}'}\left[\cos\left(\delta q_x\right) + \cos\left(\delta q_y\right)\right]\\ &\times\left[\left(\sin^2\theta_{\mathbf{q}}\tanh\left(\frac{\beta E_{\mathbf{q}}}{2}\right) + f\left(E_{\mathbf{q}};\beta,0\right)\right)\hat{c}_{\mathbf{q}'\uparrow}^{\dagger}\hat{c}_{\mathbf{q}'\uparrow}\right.\\ &\left.+ \left(1 - \cos^2\theta_{-\mathbf{q}}\tanh\left(\frac{\beta E_{-\mathbf{q}}}{2}\right) - f\left(E_{-\mathbf{q}};\beta,0\right)\right)\hat{c}_{\mathbf{q}'\downarrow}^{\dagger}\hat{c}_{\mathbf{q}'\downarrow}\right]\end{aligned} \tag{2.28}$$

Spatial inversion symmetry guarantees

$$\cos^2\theta_{-\mathbf{q}} = \cos^2\theta_{\mathbf{q}} \quad\text{as well as}\quad E_{-\mathbf{q}} = E_{\mathbf{q}}$$

By simple algebraic manipulation is easy to see:

$$\begin{aligned}1 - \cos^2\theta_{\mathbf{q}}\tanh\left(\frac{\beta E_{\mathbf{q}}}{2}\right) - f\left(E_{\mathbf{q}};\beta,0\right) &= \sin^2\theta_{\mathbf{q}}\tanh\left(\frac{\beta E_{\mathbf{q}}}{2}\right) + 1 - \tanh\left(\frac{\beta E_{\mathbf{q}}}{2}\right) - f\left(E_{\mathbf{q}};\beta,0\right)\\ &= \sin^2\theta_{\mathbf{q}}\tanh\left(\frac{\beta E_{\mathbf{q}}}{2}\right) + f\left(E_{\mathbf{q}};\beta,0\right)\end{aligned}$$

Since

$$1 - \tanh\left(\frac{x}{2}\right) - \frac{1}{e^x + 1} = \frac{1}{e^x + 1}$$

Use now:

$$\begin{aligned}\sin^2\theta_{\mathbf{q}} &= \frac{1 - \cos(2\theta_{\mathbf{q}})}{2}\\ &= \frac{1}{2} - \frac{\xi_{\mathbf{q}}}{2\sqrt{\xi_{\mathbf{q}}^2 + |\Delta_{\mathbf{q}}|^2}}\end{aligned}$$

and let:

$$g_{\mathbf{q}} \equiv \left[\frac{1}{2} - \frac{\xi_{\mathbf{q}}}{2\sqrt{\xi_{\mathbf{q}}^2 + |\Delta_{\mathbf{q}}|^2}}\right] \tanh\left(\frac{\beta}{2}\sqrt{\xi_{\mathbf{q}}^2 + |\Delta_{\mathbf{q}}|^2}\right) + f\left(\sqrt{\xi_{\mathbf{q}}^2 + |\Delta_{\mathbf{q}}|^2}; \beta, 0\right)$$

which further simplifies to

$$g_{\mathbf{q}} \equiv \frac{1}{2} - \frac{\xi_{\mathbf{q}}}{2\sqrt{\xi_{\mathbf{q}}^2 + |\Delta_{\mathbf{q}}|^2}} \tanh\left(\frac{\beta}{2}\sqrt{\xi_{\mathbf{q}}^2 + |\Delta_{\mathbf{q}}|^2}\right) \tag{2.29}$$

Thus, the original o.s. Fock term retrieved from Wick's theorem on the EHM reduces to

$$V \sum_{\langle ij \rangle} \sum_{\sigma} \left[\langle \hat{c}_{i\sigma}^\dagger \hat{c}_{j\sigma} \rangle \hat{c}_{j\sigma}^\dagger \hat{c}_{i\sigma} + \text{h.c.}\right] = \frac{2V}{L_x L_y} \sum_{\mathbf{q},\mathbf{q}'} \sum_{\sigma} \left[\cos\left(\delta q_x\right) + \cos\left(\delta q_y\right)\right] g_{\mathbf{q}} \hat{c}_{\mathbf{q}'\sigma}^\dagger \hat{c}_{\mathbf{q}'\sigma}$$

Recall now the result of Eq. (**??**),

$$\cos\left(\delta q_x\right) + \cos\left(\delta q_y\right) = \frac{1}{2} \sum_{\gamma} \varphi_{\mathbf{q}}^{(\gamma)} \varphi_{\mathbf{q}'}^{(\gamma)*} \quad \text{for } \gamma \in \{s^*, p_x, p_y, d_{x^2 - y^2}\}$$

which gives (sum over γ is intended within the aforementioned symmetries)

$$\frac{2V}{L_x L_y} \sum_{\mathbf{q},\mathbf{q}'} \sum_{\sigma} \left[\cos\left(\delta q_x\right) + \cos\left(\delta q_y\right)\right] g_{\mathbf{q}} \hat{c}_{\mathbf{q}'\sigma}^\dagger \hat{c}_{\mathbf{q}'\sigma} = \frac{V}{L_x L_y} \sum_{\mathbf{q},\mathbf{q}'} \sum_{\sigma,\gamma} \varphi_{\mathbf{q}}^{(\gamma)} \varphi_{\mathbf{q}'}^{(\gamma)*} g_{\mathbf{q}} \hat{c}_{\mathbf{q}'\sigma}^\dagger \hat{c}_{\mathbf{q}'\sigma} \tag{2.30}$$

Evidently from Eq. (2.29), $g_{\mathbf{q}}$ is an even function of the momentum, a feature that ensures

$$\frac{1}{L_x L_y} \sum_{\mathbf{q}} \varphi_{\mathbf{q}}^{(p_\ell)} g_{\mathbf{q}} = 0 \quad \text{for } \ell \in \{x, y\}$$

General result. Let us now divide the discussion in two parts. First, let us deal with the theoretical general result of the above calculations. Define the s^* and $d_{x^2-y^2}$ components as

$$g^{(s^*)} \equiv \frac{1}{L_x L_y} \sum_{\mathbf{q}} (\cos q_x + \cos q_y) g_{\mathbf{q}} \qquad g^{(d)} \equiv \frac{1}{L_x L_y} \sum_{\mathbf{q}} (\cos q_x - \cos q_y) g_{\mathbf{q}}$$

and from Eq. (2.30) we get the final form

$$\frac{2V}{L_x L_y} \sum_{\mathbf{q},\mathbf{q}'} \sum_{\sigma} \left[\cos\left(\delta q_x\right) + \cos\left(\delta q_y\right)\right] g_{\mathbf{q}} \hat{c}_{\mathbf{q}'\sigma}^\dagger \hat{c}_{\mathbf{q}'\sigma}$$
$$= V \sum_{\mathbf{q}\sigma} \left[g^{(s^*)}(\cos q_x + \cos q_y) + g^{(d)}(\cos q_x - \cos q_y)\right] \hat{c}_{\mathbf{q}\sigma}^\dagger \hat{c}_{\mathbf{q}\sigma} \tag{2.31}$$

This equation reduces fully the initial o.s. Fock component of $\hat{H}_V$ to a simpler, decoupled form. Here, similarly to what we observed for AF phase in Sec. 1.3.2, the bare bands are renormalized,

$$\tilde{\epsilon}_{\mathbf{k}} \equiv \epsilon_{\mathbf{k}} + V \left[g^{(s^*)}(\cos k_x + \cos k_y) + g^{(d)}(\cos k_x - \cos k_y)\right] \tag{2.32}$$

As is done in next paragraph, the s^* is actually a rigid t renormalization, which however requires a little care.

Pure x-wave superconductivity.   As long as we work in a precise sector ($s \oplus s^*$ as well as $d_{x^2-y^2}$) with a gap function completely contained in said symmetry sector, we can rule out the $d_{x^2-y^2}$-wave component of $g_{\mathbf{q}}$ from Eq. (2.32)

$$\frac{1}{L_x L_y} \sum_{\mathbf{q}} \varphi_{\mathbf{q}}^{(d)} g_{\mathbf{q}} = 0$$

The result above is valid only if $\Delta_{\mathbf{q}}$ is described only by a single symmetry harmonics. This is because under a rotation of angle $\pi/2$ the two functions behave differently:

$$(q_x, q_y) \rightarrow (-q_y, q_x) \quad : \quad \begin{cases} \varphi_{\mathbf{q}}^{(d)} \rightarrow -\varphi_{\mathbf{q}}^{(d)} \\ g_{\mathbf{q}} \rightarrow g_{\mathbf{q}} \end{cases}$$

The only remainder of Eq. (2.32) is its s^* part

$$\tilde{\epsilon}_{\mathbf{k}} \equiv \epsilon_{\mathbf{k}} + V g^{(s^*)}(\cos k_x + \cos k_y) \tag{2.33}$$

and since $\epsilon_{\mathbf{k}} = -2t(\cos k_x + \cos k_y)$ we obtain an equation essentially identical to the one expressing the hopping renormalization in the AF phase, Eq. (1.18). Indeed, let $w \equiv g^{(s^*)}/2$ be the new HF parameter, we get

$$\tilde{t} \equiv t - wV \tag{2.34}$$

Once again the hopping parameter shift is rigid and controlled directly by V. As done for the AF phase, we will denote the new bands as:

$$\xi_{\mathbf{k}} \rightarrow \tilde{\xi}_{\mathbf{k}} \qquad E_{\mathbf{k}} \rightarrow \tilde{E}_{\mathbf{k}}$$

2.3.4   Ground state energy and BCS condensation

BCS essentially relies on the insurgence of an effective free fermionic field, described by the Bogoliubov bands, and the condensation of Cooper pairs. Superconducting state is favored by the lowering of free energy granted by the shifting of much of the spectral weight to a lower-energy maximum [**zhou1992density**]. "Condensation energy" is simply the energy difference between the superconducting state and the normal state, and its negativity indicates instability towards superconducting order. It's pretty straightforward to derive the ground state energy for the standard BCS state. When performing Wick's contractions,

$$\begin{aligned}
\langle \hat{c}_\alpha^\dagger \hat{c}_\beta^\dagger \hat{c}_\gamma \hat{c}_\delta \rangle \sim & \ \langle \hat{c}_\alpha^\dagger \hat{c}_\beta^\dagger \rangle \hat{c}_\gamma \hat{c}_\delta + \hat{c}_\alpha^\dagger \hat{c}_\beta^\dagger \langle \hat{c}_\gamma \hat{c}_\delta \rangle - \langle \hat{c}_\alpha^\dagger \hat{c}_\beta^\dagger \rangle \langle \hat{c}_\gamma \hat{c}_\delta \rangle & \text{Cooper terms} \\
& - \langle \hat{c}_\alpha^\dagger \hat{c}_\gamma \rangle \hat{c}_\beta^\dagger \hat{c}_\delta - \hat{c}_\alpha^\dagger \hat{c}_\gamma \langle \hat{c}_\beta^\dagger \hat{c}_\delta \rangle + \langle \hat{c}_\alpha^\dagger \hat{c}_\gamma \rangle \langle \hat{c}_\beta^\dagger \hat{c}_\delta \rangle & \text{Fock terms} \\
& + \langle \hat{c}_\alpha^\dagger \hat{c}_\delta \rangle \hat{c}_\beta^\dagger \hat{c}_\gamma + \hat{c}_\alpha^\dagger \hat{c}_\delta \langle \hat{c}_\beta^\dagger \hat{c}_\gamma \rangle - \langle \hat{c}_\alpha^\dagger \hat{c}_\delta \rangle \langle \hat{c}_\beta^\dagger \hat{c}_\gamma \rangle & \text{Hartree terms}
\end{aligned}$$

Form each of the three rows above, the last term is the "leftover" part which shifts energy. Thus it can be ignored in derivation, but becomes important when considering the energy in the end. The EHM hamiltonian can be written as:

$$\hat{H} = \sum_{\mathbf{k}} \xi_{\mathbf{k}} \left[\hat{c}_{\mathbf{k}\uparrow}^\dagger \hat{c}_{\mathbf{k}\uparrow} + \mathbb{I} - \hat{c}_{-\mathbf{k}\downarrow} \hat{c}_{-\mathbf{k}\downarrow}^\dagger \right] - \sum_{\mathbf{k},\mathbf{k}'} \left[V^{(s)} + V_{\mathbf{k}\mathbf{k}'} \right] \hat{\phi}_{\mathbf{k}}^\dagger \hat{\phi}_{\mathbf{k}'}$$

$$- \frac{2V}{L_x L_y} \sum_{\mathbf{k},\mathbf{k}'} \sum_\sigma \left[\cos(\delta k_x) + \cos(\delta k_y) \right] \hat{n}_{\mathbf{k}\sigma} \hat{n}_{\mathbf{k}'\sigma} \tag{2.35}$$

as in Eq. (2.7). Following the scheme above, the "leftovers" of the MFT hamiltonian are just

$$\sum_{\mathbf{k},\mathbf{k}'} \Delta_{\mathbf{k}} \langle \hat{\phi}_{\mathbf{k}'} \rangle - \frac{2V}{L_x L_y} \sum_{\mathbf{k},\mathbf{k}'} \sum_\sigma \left[\cos(\delta k_x) + \cos(\delta k_y) \right] g_{\mathbf{k}} g_{\mathbf{k}'}$$

Further developing this result and applying Eqns. (2.17), (**??**), these last terms can be written as:

$$\sum_{\mathbf{k}} \frac{|\Delta_{\mathbf{k}}|^2}{2\tilde{E}_{\mathbf{k}}} \tanh\left(\frac{\beta \tilde{E}_{\mathbf{k}}}{2}\right) - 2V L_x L_y \sum_\gamma \left| g^{(\gamma)} \right|^2 \qquad \gamma \in \{s^*, d_{x^2-y^2}\} \tag{2.36}$$

as for Eq. (2.31). Notice the presence of a volume factor in the $\mathcal{O}\left(g^2\right)$ correction.

Now, we retrieve the expression for the MFT free energy density [**hutchinson2021mixed**] simply by adding four contributions:

1. Bogoliubov free quasiparticles thermal ground state energy density,

$$\frac{1}{L_x L_y} \sum_{\mathbf{k}} \tilde{E}_{\mathbf{k}} \left[f(\tilde{E}_{\mathbf{k}}; \beta, 0) - f(-\tilde{E}_{\mathbf{k}}; \beta, 0) \right] = \frac{1}{L_x L_y} \sum_{\mathbf{k}} \tilde{E}_{\mathbf{k}} \left[f(\tilde{E}_{\mathbf{k}}; \beta, 0) - \left(1 - f(\tilde{E}_{\mathbf{k}}; \beta, 0) \right) \right]$$

$$= \frac{2}{L_x L_y} \sum_{\mathbf{k}} \tilde{E}_{\mathbf{k}} f(\tilde{E}_{\mathbf{k}}; \beta, 0) - \frac{1}{L_x L_y} \sum_{\mathbf{k}} \tilde{E}_{\mathbf{k}}$$

   having used the simple property of the Fermi-Dirac distribution $f(-x; \beta, 0) = 1 - f(-x; \beta, 0)$.

2. The term originated by the identity produced by fermionic anticommutation rules in Eq. (2.35),

$$\frac{1}{L_x L_y} \sum_{\mathbf{k}} \tilde{\xi}_{\mathbf{k}}$$

   averaged on the lattice.

3. The "leftovers" of Eq. (2.36), divided by $L_x L_y$.

4. The entropic free energy

$$-Ts$$

   with $T = 1/k_B \beta$ and s the free Fermi gas entropy density for the Bogoliubov quasiparticles,

$$s = -\frac{2k_B}{L_x L_y} \sum_{\mathbf{k}} \left[\left(1 - f(\tilde{E}_{\mathbf{k}}; \beta, 0) \right) \ln \left(1 - f(\tilde{E}_{\mathbf{k}}; \beta, 0) \right) + f(\tilde{E}_{\mathbf{k}}; \beta, 0) \ln f(\tilde{E}_{\mathbf{k}}; \beta, 0) \right]$$

   We use the identity:

$$\ln \left(1 - \frac{1}{e^x + 1} \right) = x + \ln \left(\frac{1}{e^x + 1} \right)$$

   and reduce the above expression to:

$$s = -\frac{2k_B}{L_x L_y} \sum_{\mathbf{k}} \Big[\ln \left(1 - f(\tilde{E}_{\mathbf{k}}; \beta, 0) \right) + f(\tilde{E}_{\mathbf{k}}; \beta, 0) \ln f(\tilde{E}_{\mathbf{k}}; \beta, 0)$$

$$- \beta \tilde{E}_{\mathbf{k}} f(\tilde{E}_{\mathbf{k}}; \beta, 0) - f(\tilde{E}_{\mathbf{k}}; \beta, 0) \ln f(\tilde{E}_{\mathbf{k}}; \beta, 0) \Big]$$

   Second and fourth terms cancel out, while the third compensates the first one of contribution 1.

All together, the MFT averaged free energy looks like this:

$$f_{\text{MFT}}[\Delta_{\mathbf{k}}, g_{\mathbf{k}}] = \frac{1}{L_x L_y} \sum_{\mathbf{k}} \left[\tilde{\xi}_{\mathbf{k}} - \tilde{E}_{\mathbf{k}} + \frac{|\Delta_{\mathbf{k}}|^2}{2\tilde{E}_{\mathbf{k}}} \tanh \left(\frac{\beta \tilde{E}_{\mathbf{k}}}{2} \right) \right]$$

$$- 2V \sum_{\gamma \in \{s^*, d\}} \left| g^{(\gamma)} \right|^2 + \frac{2}{\beta L_x L_y} \sum_{\mathbf{k}} \ln \left(1 - f(\tilde{E}_{\mathbf{k}}; \beta, 0) \right) \quad (2.37)$$

The two main differences with the commonly known expressions for f_{MFT} [**hutchinson2021mixed**, **senarath2025mixed**] are the presence of bands renormalization , the absence of $-\mu n$ [Why?], and the $\mathcal{O}\left(g^2\right)$ correction. The latter, not only is negative for attractive V, a feature that can lead to superconducting phase energy lowering and stabilisation, but also it depends explicitly on the spectral amplitude of the s^* and d-wave components of $g_{\mathbf{k}}$. Since as seen the d-wave part of $g_{\mathbf{k}}$ arises for mixed symmetries, this details seems to indicate an energetic preference for multi-symmetry phases.

2.4 Results of the HF algorihtm

[To be continued...]

Appendix A

Mean-Field Theory in Hubbard lattices

In this Appendix the MFT solutions to the conventional Hubbard hamiltonian of Eq. (**??**),

$$\hat{H} = -t \sum_{\langle ij \rangle} \sum_{\sigma} \hat{c}_{i\sigma}^{\dagger} \hat{c}_{j\sigma} + U \sum_{i} \hat{n}_{i\uparrow} \hat{n}_{i\downarrow} \qquad t, U > 0 \tag{A.1}$$

are described. The discussion is limited to the two-dimensional square lattice.

A.1   Symmetries of the Hubbard model and magnetic phase transitions

The Hubbard model defined on the planar square lattice presents various natural symmetries, discussed in detail by **arovas2022hubbard** [**arovas2022hubbard**] and for the EHM in Sec. **??**. These are reported in Tab. **??**. For the conventional Hubbard model, $\hat{H}_t + \hat{H}_U$, the three essential symmetries are translational invariance, spin rotations and charge conservation. In this appendix we investigate magnetic ordering: thus we perform a SU(2) $\to$ U(1) SSB of the kind depicted in Fig. **??**, choosing a particular magnetization direction.

   As is done in Chap. **??**, the starting point is to apply Wick's theorem to reduce the quartic hamiltonian of Eq. (A.1) to a quadratic form. Considering the discussion that leads to Eq. (**??**), it's evident that for the symmetry scheme we are dealing with the Fock term in decomposition is always suppressed, as well as the Cooper term. Then we remain with just the Hartree term,

$$\hat{n}_{i\uparrow} \hat{n}_{i\downarrow} = (\langle \hat{n}_{i\uparrow} \rangle + \delta \hat{n}_{i\uparrow}) (\langle \hat{n}_{i\downarrow} \rangle + \delta \hat{n}_{i\downarrow})$$
$$\simeq \langle \hat{n}_{i\uparrow} \rangle \langle \hat{n}_{i\downarrow} \rangle + \delta \hat{n}_{i\uparrow} \langle \hat{n}_{i\downarrow} \rangle + \langle \hat{n}_{i\uparrow} \rangle \delta \hat{n}_{i\downarrow} + \mathcal{O} \left(\delta n^2 \right)$$
$$= - \langle \hat{n}_{i\uparrow} \rangle \langle \hat{n}_{i\downarrow} \rangle + \hat{n}_{i\uparrow} \langle \hat{n}_{i\downarrow} \rangle + \langle \hat{n}_{i\uparrow} \rangle \hat{n}_{i\downarrow} + \mathcal{O} \left(\delta n^2 \right)$$

where $\delta \hat{n}_{i\sigma} \equiv \hat{n}_{i\sigma} - \langle \hat{n}_{i\sigma} \rangle$ and orders higher than first have been ignored, assuming negligible fluctuations around the equilibrium single-site population. The first term of the above three can be neglected at fixed particles number, being a pure energy shift.

A.2   Ferromagnetic phase

The MFT ferromagnetic solution prescribes an uniformly magnetized lattice,

$$\langle \hat{n}_{i\uparrow} \rangle = n + m \qquad \langle \hat{n}_{i\downarrow} \rangle = n - m$$

where n is the site electron density and m is the density unbalance, leading to a magnetization per site $2m$. The mean-field hamiltonian with these substitutions becomes:

$$\hat{H} \simeq -t \sum_{\langle ij \rangle} \sum_{\sigma} \hat{c}_{i\sigma}^{\dagger} \hat{c}_{j\sigma} + U \sum_{i} [\hat{n}_{i\uparrow} \langle \hat{n}_{i\downarrow} \rangle + \langle \hat{n}_{i\uparrow} \rangle \hat{n}_{i\downarrow}]$$
$$= -t \sum_{\langle ij \rangle} \sum_{\sigma} \hat{c}_{i\sigma}^{\dagger} \hat{c}_{j\sigma} + nU \sum_{i} [\hat{n}_{i\uparrow} + \hat{n}_{i\downarrow}] - mU \sum_{i} [\hat{n}_{i\uparrow} - \hat{n}_{i\downarrow}]$$

| Depiction of the Hubbard square lattice hopping band $\epsilon_{\mathbf{k}} = -2t[\cos(k_x) + \cos(k_y)]$. The red lines mark the zero-energy intersection.

Fourier transforming,

$$-t\sum_{\langle ij \rangle}\sum_{\sigma} \hat{c}^{\dagger}_{i\sigma}\hat{c}_{j\sigma} = -2t\sum_{\mathbf{k}\sigma}[\cos(k_x) + \cos(k_y)]\,\hat{n}_{\mathbf{k}\sigma}$$

$$nU\sum_{i}[\hat{n}_{i\uparrow} + \hat{n}_{i\downarrow}] = nU\sum_{\mathbf{k}\sigma}\hat{n}_{\mathbf{k}\sigma}$$

$$mU\sum_{i}[\hat{n}_{i\uparrow} - \hat{n}_{i\downarrow}] = mU\sum_{\mathbf{k}\sigma}[\hat{n}_{\mathbf{k}\uparrow} - \hat{n}_{\mathbf{k}\downarrow}]$$

For a square lattice, the Brillouin Zone is delimited by

$$\mathbf{k} \in [-\pi, \pi] \times [-\pi, \pi]$$

The hopping single-state energy is given by

$$\epsilon_{\mathbf{k}} = -2t\left[\cos(k_x) + \cos(k_y)\right]$$

represented as a band in Fig. A.1. At $U = 0$, the mean-field ferromagnetic state fills the band bottom-up. The single-state energy becomes:

$$\epsilon_{\mathbf{k}\uparrow} = U\left(n - m\right) - 2t\left[\cos(k_x) + \cos(k_y)\right]$$
$$\epsilon_{\mathbf{k}\downarrow} = U\left(n + m\right) - 2t\left[\cos(k_x) + \cos(k_y)\right]$$

Now it is a matter of finding the optimal value for m, minimizing the total energy at fixed filling $\rho = 2n$. Notice that said minimization is performed parametrically varying the magnetization m, inside the ferromagnetic-polarized space. As it turns out, for strong local repulsion $U/t \gg 1$, antiferromagnetic ordering is preferred. Comparison is needed in order to assess which magnetic ordering is preferred.

Consider the half-filling situation. An unpolarized system will have $n = 1/4$, $m = 0$: this implies $\langle \hat{n}_{i\uparrow} \rangle = \langle \hat{n}_{i\downarrow} \rangle = 1/4$. A perfectly up-ferromagnetic system, $n = 1/4$, $m = 1/4$: then $\langle \hat{n}_{i\uparrow} \rangle = 1/2$ and $\langle \hat{n}_{i\downarrow} \rangle = 0$. [To be continued...]

A.3 Antiferromagnetic phase

Consider now an AF mean-field solution. Let us change notation, indicating each site as

$$i \rightarrow \mathbf{r} = (x, y) \qquad x, y \in \mathbb{N}$$

The mean-field AF solution at half-filling is the uniform-modulated magnetization

$$m_{\mathbf{r}} = (-1)^{x+y}m \qquad m \in [-1, 1]$$

and a mean-field Ansatz

$$\langle \hat{n}_{\mathbf{r}\uparrow} \rangle = n + m_{\mathbf{r}} \qquad \langle \hat{n}_{\mathbf{r}\downarrow} \rangle = n - m_{\mathbf{r}} \tag{A.2}$$

In next sections, the details of the MFT solution are discussed.

A.3.1 MFT discussion

With respect to the ferromagnetic solution presented above, the only detail changing is the last term,

$$\hat{H} = -t\sum_{\langle \mathbf{rr'} \rangle}\sum_{\sigma} \hat{c}^{\dagger}_{\mathbf{r}\sigma}\hat{c}_{\mathbf{r'}\sigma} + nU\sum_{\mathbf{r}}[\hat{n}_{\mathbf{r}\uparrow} + \hat{n}_{\mathbf{r}\downarrow}] - mU\sum_{\mathbf{r}}(-1)^{x+y}[\hat{n}_{\mathbf{r}\uparrow} - \hat{n}_{\mathbf{r}\downarrow}] \tag{A.3}$$

Figure A.2 | Alternative depiction of the Hubbard square lattice hopping band previously reported in Fig. A.1. The Magnetic Brillouin Zone (MBZ) is delimited by the zero-energy contour and is indicated in figure. As it is evident, energy sign flips by taking a (π, π) translation in **k** space.

Fourier-transforming, the phase factor can be absorbed in the destruction operator inside of $\hat{n}_{\mathbf{r}\sigma}$:

$$\sum_{\mathbf{r}} (-1)^{x+y} \hat{n}_{\mathbf{r}\sigma} = \sum_{\mathbf{r}} (-1)^{x+y} \hat{c}^{\dagger}_{\mathbf{r}\sigma} \hat{c}_{\mathbf{r}\sigma}$$

$$= \sum_{\mathbf{r}} e^{i\boldsymbol{\pi}\cdot\mathbf{r}} \frac{1}{\sqrt{L_x L_y}} \sum_{\mathbf{k}\in\text{BZ}} e^{i\mathbf{k}\cdot\mathbf{r}} \hat{c}^{\dagger}_{\mathbf{k}\sigma} \frac{1}{\sqrt{L_x L_y}} \sum_{\mathbf{k}'\in\text{BZ}} e^{-i\mathbf{k}'\cdot\mathbf{r}} \hat{c}_{\mathbf{k}'\sigma}$$

$$= \sum_{\mathbf{k}\in\text{BZ}} \sum_{\mathbf{k}'\in\text{BZ}} \hat{c}^{\dagger}_{\mathbf{k}\sigma} \hat{c}_{\mathbf{k}'\sigma} \frac{1}{L_x L_y} \sum_{\mathbf{r}} e^{-i[\mathbf{k}'-(\mathbf{k}+\boldsymbol{\pi})]\cdot\mathbf{r}}$$

$$= \sum_{\mathbf{k}\in\text{BZ}} \hat{c}^{\dagger}_{\mathbf{k}\sigma} \hat{c}_{\mathbf{k}+\boldsymbol{\pi}\sigma}$$

where $\boldsymbol{\pi} = (\pi, \pi)$. It follows:

$$mU \sum_{\mathbf{r}} (-1)^{x+y} [\hat{n}_{\mathbf{r}\uparrow} - \hat{n}_{\mathbf{r}\downarrow}] = \Delta \sum_{\mathbf{k}\in\text{BZ}} \left[\hat{c}^{\dagger}_{\mathbf{k}\uparrow} \hat{c}_{\mathbf{k}+\boldsymbol{\pi}\uparrow} - \hat{c}^{\dagger}_{\mathbf{k}\downarrow} \hat{c}_{\mathbf{k}+\boldsymbol{\pi}\downarrow} \right] \quad \text{where} \quad \Delta \equiv mU$$

Consider the band of Fig. A.1 at half-filling. As does **fabrizio2022course** [**fabrizio2022course**], the area delimited externally by the solid lines at zero energy is denominated "Magnetic Brillouin Zone" (MBZ). The periodicity of **k** space guarantees that the full BZ can be taken as well to be the one of Fig. **??**. Then:

$$\sum_{\mathbf{k}\in\text{BZ}} \hat{c}^{\dagger}_{\mathbf{k}\uparrow} \hat{c}_{\mathbf{k}+\boldsymbol{\pi}\uparrow} = \sum_{\mathbf{k}\in\text{MBZ}} \left[\hat{c}^{\dagger}_{\mathbf{k}\uparrow} \hat{c}_{\mathbf{k}+\boldsymbol{\pi}\uparrow} + \hat{c}^{\dagger}_{\mathbf{k}+\boldsymbol{\pi}\uparrow} \hat{c}_{\mathbf{k}+2\boldsymbol{\pi}\uparrow} \right]$$

$$= \sum_{\mathbf{k}\in\text{MBZ}} \left[\hat{c}^{\dagger}_{\mathbf{k}\uparrow} \hat{c}_{\mathbf{k}+\boldsymbol{\pi}\uparrow} + \hat{c}^{\dagger}_{\mathbf{k}+\boldsymbol{\pi}\uparrow} \hat{c}_{\mathbf{k}\uparrow} \right] \tag{A.4}$$

and the same applies for spin $\downarrow$. Periodicity by shifts $2\boldsymbol{\pi}$ has been used. Now, define the Nambu spinors:

$$\hat{\Psi}_{\mathbf{k}\sigma} \equiv \begin{bmatrix} \hat{c}_{\mathbf{k}\sigma} \\ \hat{c}_{\mathbf{k}+\boldsymbol{\pi}\sigma} \end{bmatrix}$$

and a spin-wise gap,

$$\Delta_{\uparrow} = \Delta \qquad \Delta_{\downarrow} = -\Delta$$

At fixed filling, the nU term is a pure chemical potential shift, thus will be neglected. The kinetic term transforms as

$$-t \sum_{\langle ij \rangle} \sum_{\sigma} \hat{c}^{\dagger}_{i\sigma} \hat{c}_{j\sigma} = \sum_{\mathbf{k}\in\text{BZ}} \sum_{\sigma} \epsilon_{\mathbf{k}} \hat{c}^{\dagger}_{\mathbf{k}\sigma} \hat{c}_{\mathbf{k}\sigma}$$

$$= \sum_{\mathbf{k}\in\text{MBZ}} \sum_{\sigma} \left[\epsilon_{\mathbf{k}} \hat{c}^{\dagger}_{\mathbf{k}\sigma} \hat{c}_{\mathbf{k}\sigma} + \epsilon_{\mathbf{k}+\boldsymbol{\pi}} \hat{c}^{\dagger}_{\mathbf{k}+\boldsymbol{\pi}\sigma} \hat{c}_{\mathbf{k}+\boldsymbol{\pi}\sigma} \right]$$

$$= \sum_{\mathbf{k}\in\text{MBZ}} \sum_{\sigma} \epsilon_{\mathbf{k}} \left[\hat{c}^{\dagger}_{\mathbf{k}\sigma} \hat{c}_{\mathbf{k}\sigma} - \hat{c}^{\dagger}_{\mathbf{k}+\boldsymbol{\pi}\sigma} \hat{c}_{\mathbf{k}+\boldsymbol{\pi}\sigma} \right]$$

In the second passage, the sum over the full BZ was written considering that the entirety of the zone is given by all the points in the MBZ plus their conjugates obtained by a $\boldsymbol{\pi}$ shift in the flipped band. As depicted in Fig. **??**, kinetic energy is anti-periodic in **k** space by a vector $\boldsymbol{\pi}$. This anti-periodicity accounts for the minus sign arising in the third passage. The hamiltonian is then given by:

$$\hat{H} = \sum_{\mathbf{k}\in\text{MBZ}} \sum_{\sigma} \hat{\Psi}^{\dagger}_{\mathbf{k}\sigma} h_{\mathbf{k}\sigma} \hat{\Psi}_{\mathbf{k}\sigma} \quad \text{being} \quad h_{\mathbf{k}\sigma} \equiv \begin{bmatrix} \epsilon_{\mathbf{k}} & -\Delta_{\sigma} \\ -\Delta_{\sigma} & -\epsilon_{\mathbf{k}} \end{bmatrix} \tag{A.5}$$

Figure A.3 | Pseudo-magnetic field originating from mean-field treatment of the square Hubbard hamiltonian. Here, only the $\sigma = \uparrow$ situation is plotted.

Notice: the Nambu hamiltonian is a 2×2 matrix over the MBZ – which is half the full BZ, coherently with a solution which essentially bipartites the lattice giving back a double sized unit cell.

A.3.2   Diagonalization and AF ground state

The system ground-state is obtained by the means of a Bogoliubov rotation. The hamiltonian maps onto the simple one of a spin in a magnetic field,

$$h_{\mathbf{k}\sigma} = \epsilon_{\mathbf{k}}\tau^z - \Delta_\sigma \tau^x$$

being τ^α the Pauli matrices. Then, defining

$$\hat{s}^\alpha_{\mathbf{k}\sigma} \equiv \hat{\Psi}^\dagger_{\mathbf{k}\sigma} \tau^\alpha \hat{\Psi}_{\mathbf{k}\sigma} \quad \text{and} \quad \mathbf{b}_{\mathbf{k}\sigma} \equiv \begin{bmatrix} -\Delta_\sigma \\ 0 \\ \epsilon_{\mathbf{k}} \end{bmatrix}$$

one gets:

$$\hat{H} = \sum_{\mathbf{k}\in\text{MBZ}} \sum_\sigma \mathbf{b}_{\mathbf{k}\sigma} \cdot \hat{\mathbf{s}}_{\mathbf{k}\sigma} \quad \text{where} \quad \hat{\mathbf{s}}_{\mathbf{k}\sigma} = \begin{bmatrix} \hat{s}^x_{\mathbf{k}\sigma} \\ \hat{s}^y_{\mathbf{k}\sigma} \\ \hat{s}^z_{\mathbf{k}\sigma} \end{bmatrix} \tag{A.6}$$

The hamiltonian represents a system of spins subject to local magnetic fields, each tilted by an angle $\tan(2\theta_{\mathbf{k}\sigma}) = \Delta_\sigma/\epsilon_{\mathbf{k}}$, as sketched in Fig. A.3. At any finite temperature, the ground-state of such a system is well-known. Diagonalization of each $h_{\mathbf{k}\sigma}$ is obtained trivially by a simple rotation around the y axis:

$$d_{\mathbf{k}\sigma} = W_{\mathbf{k}\sigma} h_{\mathbf{k}\sigma} W^\dagger_{\mathbf{k}\sigma}$$

where

$$d_{\mathbf{k}\sigma} = \begin{bmatrix} -E_{\mathbf{k}} & \\ & E_{\mathbf{k}} \end{bmatrix} \quad \text{and} \quad W_{\mathbf{k}\sigma} = \exp\left\{ i\frac{2\theta_{\mathbf{k}\sigma} - \pi}{2}\tau^y \right\}$$

Note that rotation is taken to be of an angle $2\theta_{\mathbf{k}\sigma} - \pi$ in order to anti-align the pseudo-spin with the magnetic field of Fig. A.3 and thus order the eigenvalues as in $d_{\mathbf{k}\sigma}$, with the smaller one in the top-left corner of the matrix and the larger one in the bottom-right corner. The explicit form of the transformation matrix is thus

$$W_{\mathbf{k}\sigma} = \begin{bmatrix} \cos\theta_{\mathbf{k}\sigma} & -\sin\theta_{\mathbf{k}\sigma} \\ \sin\theta_{\mathbf{k}\sigma} & \cos\theta_{\mathbf{k}\sigma} \end{bmatrix} \begin{bmatrix} & -1 \\ 1 & \end{bmatrix} = \begin{bmatrix} -\sin\theta_{\mathbf{k}\sigma} & -\cos\theta_{\mathbf{k}\sigma} \\ \cos\theta_{\mathbf{k}\sigma} & -\sin\theta_{\mathbf{k}\sigma} \end{bmatrix} \tag{A.7}$$

Eigenvalues are:

$$E_{\mathbf{k}} \equiv \sqrt{\epsilon_{\mathbf{k}}^2 + |\Delta_\sigma|^2} \tag{A.8}$$

Note that considering the full hamiltonian $\hat{H} - \mu\hat{N}$, the diagonalizing matrix remains the same, being

$$-\mu\hat{N} = \sum_{\mathbf{k}\in\text{MBZ}} \begin{bmatrix} -\mu & \\ & -\mu \end{bmatrix} \quad \implies \quad W_{\mathbf{k}\sigma}\left[h_{\mathbf{k}\sigma} - \mu\mathbb{I}_{2\times 2}\right]W^\dagger_{\mathbf{k}\sigma} = d_{\mathbf{k}\sigma} - \mu\mathbb{I}_{2\times 2} \tag{A.9}$$

thus for non-null chemical potential (i.e. finite doping) the eigenvalues are just shifted, $\pm E_{\mathbf{k}} - \mu$. In other words, the new bands retain the same chemical potential of the bare bands. Notice also that the presence of an absolute value makes the eigenvalues independent of the σ index. Eigenvector fermion operators are obtained simply as:

$$\hat{\Gamma}_{\mathbf{k}\sigma} = W_{\mathbf{k}\sigma}\hat{\Psi}_{\mathbf{k}\sigma} \tag{A.10}$$

The $\hat{\Gamma}$ spinor operators are effectively free fermionic spinor fields and as such must be treated.

The consequence of Eq. (A.9) is interesting by itself: within this HF solution, the gap opens always at $E = 0$. In other words, the bands sketched in Fig. A.4 retain the same geometric features regardless of the doping, what changes is the bands width and the gap between them. The very key point here is that, being the two bands symmetric (thus containing each half of the electronic states) and defined over the MBZ, any finite doping $\delta > 0$ will produce a metallic behaviour, imposing that the chemical potential crosses the upper band. It is widely observed and confirmed by more refined numerical procedures, however, that AF establishes an insulating phase – here only reproduced at half-filling, where the chemical potential lies within the gap. As will be detailed in A.3.6, the commensurate nature of AF SSB at wavevector $\boldsymbol{\pi}$ of this self-consistent solution is highly unstable and atypical at finite doping [**singh1990collective**].

A.3.3   Chemical potential and system density

The total number of electrons is given by

$$
\begin{aligned}
N &= \sum_{\mathbf{k}\sigma} \langle \hat{n}_{\mathbf{k}\sigma} \rangle \\
&= \sum_{\sigma} \sum_{\mathbf{k}\in\text{MBZ}} \langle \hat{n}_{\mathbf{k}\sigma} + \hat{n}_{\mathbf{k}+\boldsymbol{\pi}\sigma} \rangle \\
&= \sum_{\sigma} \sum_{\mathbf{k}\in\text{MBZ}} \left\langle \hat{\Gamma}^{\dagger}_{\mathbf{k}\sigma} \hat{\Gamma}_{\mathbf{k}\sigma} \right\rangle \\
&= 2 \sum_{\mathbf{k}\in\text{MBZ}} \left[f\left(-E_{\mathbf{k}}; \beta, \mu\right) + f\left(E_{\mathbf{k}}; \beta, \mu\right) \right]
\end{aligned}
\tag{A.11}
$$

being f be the Fermi-Dirac distribution at inverse temperature β and chemical potential μ,

$$
f(\epsilon; \beta, \mu) = \frac{1}{e^{\beta(\epsilon - \mu)} + 1}
$$

The 2 prefactor appeared because of spin degeneracy. Since the gapped bands refer to the smaller MBZ, thus exhibit the periodicity

$$
E_{\mathbf{k}} = E_{\mathbf{k}+\boldsymbol{\pi}}
$$

it holds equivalently

$$
N = \sum_{\mathbf{k}\in\text{BZ}} \left[f\left(-E_{\mathbf{k}}; \beta, \mu\right) + f\left(E_{\mathbf{k}}; \beta, \mu\right) \right]
\tag{A.12}
$$

as is obvious. The 2 prefactor was absorbed in doubling the integration region, MBZ $\to$ BZ. Next sections are devoted to simplify the above theoretical results in order to obtain an algorithmic estimation for the magnetization m, which is just the AF instability order parameter.

In Fig. A.5 the density $n(\mu)$ is plotted as a function of μ. As is evident, at nearly zero temperature ($\beta \to \infty$) the system is half filled for $-\Delta < \mu < \Delta$. In order to obtain a finite doping, it must be $|\mu| > \Delta$; which means, the chemical potential needs to cross the electronic bands. This HF solution leads invariably to a rather unusual metallic AF at any finite doping.

A.3.4   Self-consistent magnetization

A convergence algorithm can be designed to find the Hartree-Fock solution to the model. Ultimately, we aim to extract m self-consistently. Since

$$
\begin{aligned}
m &= \frac{1}{2L_x L_y} \sum_{\mathbf{r}} (-1)^{x+y} \langle \hat{n}_{\mathbf{r}\uparrow} - \hat{n}_{\mathbf{r}\downarrow} \rangle \\
&= \frac{1}{2L_x L_y} \sum_{\mathbf{k}\in\text{BZ}} \left\langle \hat{c}^{\dagger}_{\mathbf{k}\uparrow} \hat{c}_{\mathbf{k}+\boldsymbol{\pi}\uparrow} - \hat{c}^{\dagger}_{\mathbf{k}\downarrow} \hat{c}_{\mathbf{k}+\boldsymbol{\pi}\downarrow} \right\rangle \\
&= \frac{1}{2L_x L_y} \sum_{\mathbf{k}\in\text{MBZ}} \left\langle \left(\hat{c}^{\dagger}_{\mathbf{k}\uparrow} \hat{c}_{\mathbf{k}+\boldsymbol{\pi}\uparrow} + \hat{c}^{\dagger}_{\mathbf{k}+\boldsymbol{\pi}\uparrow} \hat{c}_{\mathbf{k}\uparrow} \right) - \left(\hat{c}^{\dagger}_{\mathbf{k}\downarrow} \hat{c}_{\mathbf{k}+\boldsymbol{\pi}\downarrow} + \hat{c}^{\dagger}_{\mathbf{k}+\boldsymbol{\pi}\downarrow} \hat{c}_{\mathbf{k}\downarrow} \right) \right\rangle
\end{aligned}
$$
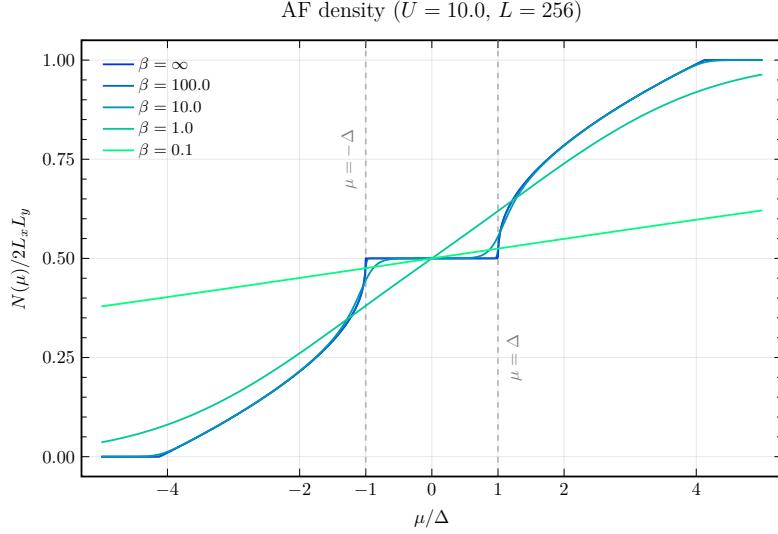
Figure A.5 | Electronic density in the AF phase as a function of the chemical potential, measured in relation to the gap Δ, at various temperatures.

In the last passage, Eq. (A.4) has been used. Then magnetization can be computed simply as

$$m = \frac{1}{2L_x L_y} \sum_{\mathbf{k} \in \mathrm{MBZ}} \left[\left\langle \hat{\Psi}_{\mathbf{k}\uparrow}^{\dagger} \tau^x \hat{\Psi}_{\mathbf{k}\uparrow} \right\rangle - \left\langle \hat{\Psi}_{\mathbf{k}\downarrow}^{\dagger} \tau^x \hat{\Psi}_{\mathbf{k}\downarrow} \right\rangle \right] \tag{A.13}$$

In this equation, spin expectation values appear:

$$\left\langle \hat{\Psi}_{\mathbf{k}\sigma}^{\dagger} \tau^x \hat{\Psi}_{\mathbf{k}\sigma} \right\rangle = \langle \hat{s}_{\mathbf{k}\sigma}^x \rangle$$

Now discussion is divided in two parts: zero temperature and finite temperature.

Zero temperature solution. For a spin system at zero temperature, the spin operator expectation value anti-aligns with the external field,

$$\langle \hat{s}_{\mathbf{k}\sigma}^x \rangle = \sin(2\theta_{\mathbf{k}\sigma})$$

(see Fig. A.3). Now, since $\Delta_\downarrow = -\Delta_\uparrow$, it follows

$$\theta_{\mathbf{k}\uparrow} = -\theta_{\mathbf{k}\downarrow} \equiv \theta_{\mathbf{k}}$$

Then, from Eq. (A.13)

$$m = \frac{1}{L_x L_y} \sum_{\mathbf{k} \in \mathrm{MBZ}} \sin(2\theta_{\mathbf{k}})$$

$$= \frac{1}{2L_x L_y} \sum_{\mathbf{k} \in \mathrm{BZ}} \sin(2\theta_{\mathbf{k}})$$

The last passage is due to the fact that the sum over the MBZ can be performed identically over $\mathrm{BZ} \setminus \mathrm{MBZ}$ and yield the same result. This is because of the lattice periodicity in reciprocal space. Then, finally:

$$m = \frac{1}{L_x L_y} \sum_{\mathbf{k} \in \mathrm{BZ}} [W_{\mathbf{k}\uparrow}]_{11} [W_{\mathbf{k}\uparrow}^{\dagger}]_{21} \tag{A.14}$$

where $\sin(2\theta_{\mathbf{k}}) = 2 \sin\theta_{\mathbf{k}} \cos\theta_{\mathbf{k}}$ has been used. As will become clear in next section, the sudden appearance of matrix elements of W is not casual.

Finite temperature solution. At finite temperature β, discussion is analogous to the section above. Here will be treated somewhat more theoretically. Define the generic order parameter:

$$\Delta_{ij}(\mathbf{k}\sigma) \equiv \left\langle [\hat{\Psi}^\dagger_{\mathbf{k}\sigma}]_i [\hat{\Psi}_{\mathbf{k}\sigma}]_j \right\rangle$$

In last section, the relevant indices (i, j) were $(1, 2)$ and $(2, 1)$. Transform this order parameter,

$$
\begin{aligned}
\Delta_{ij}(\mathbf{k}\sigma) &= \sum_{i'j'} \left\langle [\hat{\Gamma}^\dagger_{\mathbf{k}\sigma}]_{i'} [W_{\mathbf{k}\sigma}]_{i'i} [W^\dagger_{\mathbf{k}\sigma}]_{jj'} [\hat{\Gamma}_{\mathbf{k}\sigma}]_{j'} \right\rangle \\
&= \sum_{i'j'} [W_{\mathbf{k}\sigma}]_{i'i} [W^\dagger_{\mathbf{k}\sigma}]_{jj'} \left\langle [\hat{\Gamma}^\dagger_{\mathbf{k}\sigma}]_{i'} [\hat{\Gamma}_{\mathbf{k}\sigma}]_{j'} \right\rangle \\
&= \sum_{i'j'} [W_{\mathbf{k}\sigma}]_{i'i} [W^\dagger_{\mathbf{k}\sigma}]_{jj'} \delta_{i'j'} f\left([d_{\mathbf{k}\sigma}]_{i'i'}; \beta, \mu\right) \\
&= \sum_{\ell=1}^{2} [W_{\mathbf{k}\sigma}]_{\ell i} [W^\dagger_{\mathbf{k}\sigma}]_{j\ell} f\left((-1)^\ell E_{\mathbf{k}\sigma}; \beta, \mu\right) \\
&= [W_{\mathbf{k}\sigma}]_{1i} [W^\dagger_{\mathbf{k}\sigma}]_{j1} f\left(-E_{\mathbf{k}}; \beta, \mu\right) + [W_{\mathbf{k}\sigma}]_{2i} [W^\dagger_{\mathbf{k}\sigma}]_{j2} f\left(E_{\mathbf{k}}; \beta, \mu\right) \quad \text{(A.15)}
\end{aligned}
$$

In the second passage this distribution appeared because an expectation value over a gas of free Φ fermions was taken. Such an expectation value admits no off-diagonal values, hence the $\delta_{i'j'}$. The diagonal entries are precisely the definition of the Fermi-Dirac distribution for the given energy. At zero temperature and half-filling, the lower band $-E_{\mathbf{k}}$ is completely filled while the upper band $E_{\mathbf{k}}$ is empty. Substituting $f = 1$ in the first term of line (A.15), $f = 0$ in the second and summing Δ_{12} and Δ_{21} as done in Eq. (A.13), it's easy to derive the result of Eq. (A.14). At finite temperature, following the lead of the above paragraph, the antiferromagnetic instability order parameter m will be given simply by

$$m = \frac{1}{2L_x L_y} \sum_{\mathbf{k} \in \text{BZ}} \sum_{\ell=1}^{2} [W_{\mathbf{k}\uparrow}]_{\ell 1} [W^\dagger_{\mathbf{k}\uparrow}]_{2\ell} f\left((-1)^\ell E_{\mathbf{k}}; \beta, \mu\right) \quad \text{(A.16)}$$

Then: mean-field approximations yield an estimate for the magnetization at a given temperature and chemical potential just by carefully combining the elements of the diagonalizing matrix W of each Bogoliubov matrix $h_{\mathbf{k}\sigma}$.

A.3.5 The half-filled case

Consider specifically the half-filled situation. Since due to symmetry $\mu = 0$, we have the finite-temperature self-consistent equation

$$
\begin{aligned}
m &= \frac{1}{L_x L_y} \sum_{\mathbf{k} \in \text{MBZ}} \sin(2\theta_{\mathbf{k}}) \left[f\left(-E_{\mathbf{k}}; \beta, 0\right) - f\left(E_{\mathbf{k}}; \beta, 0\right) \right] \\
&= \frac{1}{2L_x L_y} \sum_{\mathbf{k} \in \text{MBZ}} \frac{\Delta}{\sqrt{\epsilon_{\mathbf{k}}^2 + \Delta^2}} \tanh\left(\frac{\beta}{2}\sqrt{\epsilon_{\mathbf{k}}^2 + \Delta^2}\right)
\end{aligned}
$$

Recalling that $m = \Delta/U$, the above equation becomes in thermodynamic limit $L \to \infty$

$$\frac{1}{U} \simeq \frac{1}{2} \int_{\text{MBZ}} \frac{d\mathbf{k}}{(2\pi)^2} \frac{1}{\sqrt{\epsilon_{\mathbf{k}}^2 + \Delta^2}} \tanh\left(\frac{\beta}{2}\sqrt{\epsilon_{\mathbf{k}}^2 + \Delta^2}\right)$$

Substitute the momentum integral with an integral over energies, in the low temperature limit, $\beta \to \infty$ (thus approximate the hyperbolic tangent with 1)

$$\frac{1}{U} \simeq \frac{1}{2} \int_{\text{bands}} \frac{d\epsilon \rho(\epsilon)}{\sqrt{\epsilon^2 + \Delta^2}}$$

[To be continued...]

A.3.6 Instability of the commensurate AF solution and atypical metallic bands

A key point to be discussed is the known instability of the AF HF solution of the EHM. As is thoroughly discussed in [**singh1990collective**], the solution we presented above is only stable at half-filling, becoming hardly unstable at infinitesimal doping. This is due to the commensurate nature of the established AF phase: we impose SSB to take place at wavevector $\boldsymbol{\pi}$, shrinking the BZ to exactly half its size and giving back on the newly defined MBZ two bands $\pm E_{\mathbf{k}}$. This procedure actually works well for the half-filled case: the magnetization essentially depends on the scattering rate between points on the FS connected by a $\boldsymbol{\pi}$ vector. The half filled case, taking advantage of the natural nesting property of the bare bands,

$$\forall \mathbf{k} \in \partial\mathrm{MBZ} : \ \epsilon_{\mathbf{k}} = \epsilon_{\mathbf{k}+\boldsymbol{\pi}}$$

(being $\partial\mathrm{MBZ}$ the boundary of the MBZ) exhibits a magnetization at infinitesimal interaction. For a many body state resulting from continuous SSB, to establish a given phase means to show the presence of a stable gapless Goldstone mode associated to the broken symmetry. Such a Goldstone mode is essentially a sharp peak at zero frequency for some dressed response function. For the AF phase, it follows from the reduced $\mathrm{U}^z(1)$ rotational symmetry and is related to the proper transverse pseudospin-pseudospin response function, 2×2 matrix equation,

$$\tilde{\chi}_{\hat{\mathbf{S}}^-\hat{\mathbf{S}}^+}(\mathbf{k},\omega) = \frac{\chi_{\hat{\mathbf{S}}^-\hat{\mathbf{S}}^+}(\mathbf{k},\omega)}{1 - U\chi_{\hat{\mathbf{S}}^-\hat{\mathbf{S}}^+}(\mathbf{k},\omega)} \tag{A.17}$$

being χ the free transverse response. The pseudospin hereby considered is the one of Eq. (A.6). As is shown in [**singh1990collective**], for the commensurate AF SSB at wavevector $\boldsymbol{\pi}$ the condition for the presence of a stable gapless mode reduces to a 2×2 matrix equation,

$$\text{Stability condition:} \qquad \mathbb{I}_{2\times2} - U\left[\chi_{\hat{\mathbf{S}}^-\hat{\mathbf{S}}^+}(\boldsymbol{\pi},0)\right] \geq 0 \tag{A.18}$$

with $\left[\chi_{\hat{\mathbf{S}}^-\hat{\mathbf{S}}^+}(\boldsymbol{\pi},\omega)\right]$ the response function matrix obtained by considering a matrix response function for a two-sites unit cell. The above equation is to be interpreted as a matricial equation [Explain better..]. Considering the eigenvalue of largest amplitude of the matrix λ_δ at filling δ, the one most prone to instabilities, it is found that

$$\lambda_0(\mathbf{k} \to \boldsymbol{\pi}, 0) = \frac{1}{U} \qquad\qquad \text{(half filling)}$$

$$\lambda_\delta(\mathbf{k} \to \boldsymbol{\pi}, 0) = \frac{1}{U} + \frac{2\epsilon_{\mathrm{F}}}{\Delta}N(\epsilon_{\mathrm{F}}) \quad \text{(finite doping)}$$

The reason for the distinction above is the intrinsic metallic nature of the system for infinitesimal doping. At half-filling the system is an insulator, therefore no Fermi energy is defined, as well as no FS. Evidently this implies

$$1 - U\lambda_0(\mathbf{k} \to \boldsymbol{\pi}, 0) = 0 \quad \text{(half filling)} \qquad \implies \qquad \text{stable Goldstone mode}$$

$$1 - U\lambda_\delta(\mathbf{k} \to \boldsymbol{\pi}, 0) < 0 \quad \text{(finite doping)} \qquad \implies \qquad \text{unstable Goldstone mode}$$

For any finite doping, the commensurate AF phase becomes unstable and is destroyed by transverse spin fluctuations. Nevertheless, for the sake of completeness and because we noticed too late, we will study the metallic AF also at finite doping.

A.3.7 Hartree-Fock algorithm results in reciprocal space

The above sections offer a self-consistency equation for the magnetization m; W is determined by m indeed. Then a self-consistent algorithm to search for a self consistent estimate for m may be sketched, following the general idea of Sec. **??**:

0. Algorithm setup: initialize a counter $i = 1$ and choose:

    • the local repulsion U/t or equivalently the hopping amplitude t/U;

- the coarse-graining of the BZ, which is, fix L_x and L_y. Then

$$k_x = 2\pi n_x/L_x \qquad k_y = 2\pi n_y/L_y$$

  where $-L_j/2 \leq n_j \leq L_j/2$, $n_j \in \mathbb{Z}$;
- the density n or equivalently the doping $\delta \equiv n - 0.5$;
- the inverse temperature β;
- the number of iterations $p \in \mathbb{N}$;
- the mixing parameter $g \in [0, 1]$;
- the tolerance parameters $\Delta_m, \Delta_n \in \mathbb{R}$ (respectively for magnetization and density);

1. Select a random starting value $m_0 \in [0, 1]$;

2. For each slot of the BZ, initialize the appropriate 2×2 matrix $h_{\mathbf{k}\uparrow}$ as in Eq. (A.5);

3. For the given hamiltonian, find the optimal chemical potential μ as follows:

   a) Diagonalize $h_{\mathbf{k}\uparrow}[m_0, U]$ and obtain its eigenvalues $\pm E_{\mathbf{k}}[m_0, U]$;

   b) Define the function of the chemical potential μ,

   $$\delta n(\mu; \beta, m_0, U) \equiv 2\left[f\left(-E_{\mathbf{k}}[U, m_0]; \beta, \mu\right) + f\left(E_{\mathbf{k}}[U, m_0]; \beta, \mu\right)\right] - n$$

   c) Find the root of δn,

   $$\delta n(\mu_0) = 0$$

   Then μ_0 is the chemical potential which, at magnetization m_0, realizes the best approximation of density n;

4. Diagonalize the matrix $h_{\mathbf{k}\uparrow}$ and obtain $d_{\mathbf{k}\uparrow}$;

5. Compute m using Eq. (A.16) with chemical potential μ_0 and update the counter, $i \to i + 1$;

6. Check if $|m - m_0| \leq \delta_m$:

   - If yes, halt;
   - If not: check if $i > p$
     - If yes, halt and consider choosing better tolerance and model parameters;
     - If not, define

     $$m_0 = gm + (1 - g)m_0$$

   (logical assignment notation used) and repeat from step 2.

The algorithm sketched hereby was ran with the following setup:

```
1  UU = [U for U in 0.5:0.5:20.0]      # Local repulsions
2  LL = [256]                          # Lattice sizes
3  dd = [d for d in 0.0:0.05:0.45]     # Dopings
4  bb = [100.0, Inf]                   # Inverse temperatures
5  p = 100                             # Max number of iterations
6  dm = 1e-4                           # Tolerance on magnetization
7  dn = 1e-2                           # Tolerance on density
8  g = 0.5                             # Mixing parameter
```

In Fig. A.6 plots at $\beta = 100$ of the magnetization m is reported. As is evident in Fig. A.6a, doping disrupts AF ordering; the horizontal asymptote lowers as δ gets bigger, a mere consequence of the fact that the free space at each single-particle state in k-space shrinks as density increases; also, for $\delta > 0$, a finite magnetization m exists only for $U \geq U_c[\delta]$ (a critical value parametrically dependent on doping). Fig. A.6b shows the dependence of magnetization on doping at various fixed local repulsions U: once again, to dope the material disrupt AF ordering. Identical analysis have been performed for different temperatures, leading to analogous results as long as $\beta \gtrsim 10$ and to $m \simeq 0$ for higher temperatures (predictably).

a | Local repulsion U/t depencence.   b | Doping $\delta = n - 0.5$ dependence.
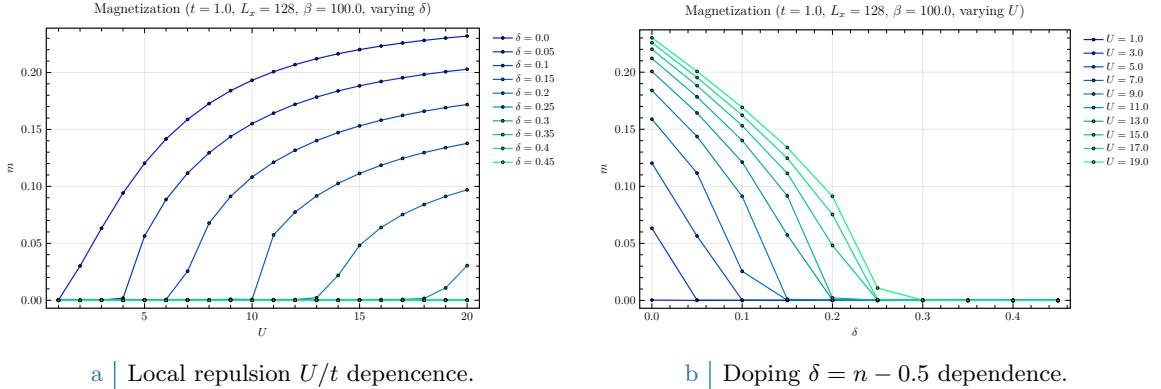
Figure A.6 | Plots of the zero-temperature AF instability order parameter m as a function of both the local repulsion U/t (Fig. A.6a) and the doping $\delta = n - 1/2$ (Fig. A.6b).
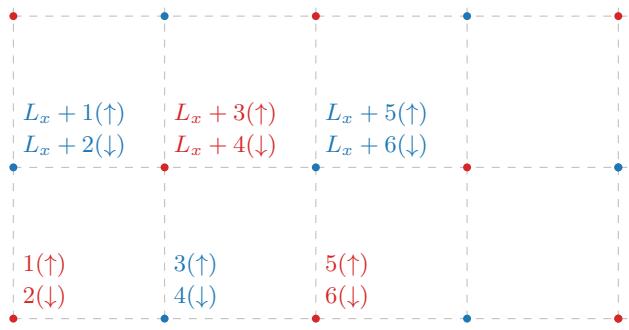

Figure A.7 | Schematics of the site ordering on a square lattice performed by sweeping along rows. Left-bottom side is one corner of the lattice. Red sites are characterized by $x + y$ being odd, blue sites by being even. The number reported near to each site is the α entry in the matrix representation for a finite square lattice.

A.3.8   An alternative (less efficient) real-space approach

The theoretical derivation of the above paragraphs offers a simple description of the system anti-ferromagnetic instability as the instauration of a ground-state of quasiparticles. Here a self-consistent algorithmic extraction of the expected magnetization is presented, following [**scholle2023comprehensive**]. Note that this algorithm is by far the least efficient, being performed in real space with dimensional exponential scaling in terms of computational time. It is here presented just for completeness as an alternative derivation. This algorithm can become useful for simulations not preserving space-translational invariance, e.g. introducing some degree of disorder. Consider a square lattice of $L_x \times L_y$ sites: the hamiltonian will be a matrix of dimension $2L_x L_y \times 2L_x L_y$,

$$[\hat{H}]_{(\mathbf{r}\sigma)(\mathbf{r}'\sigma')} = \langle \Omega | \hat{c}_{\mathbf{r}\sigma} \hat{H} \hat{c}^\dagger_{\mathbf{r}'\sigma'} | \Omega \rangle$$

For simplicity, in the following $D \equiv 2L_x L_y$. In this context, the following convention is used: the rows/column index entry $\alpha = (\mathbf{r}\sigma)$ is associated to a specific site $\mathbf{r} = (x, y)$ and spin σ through the relation

$$\alpha = 2j_{\mathbf{r}} - \delta_{\sigma=\uparrow} \quad \text{where} \quad j_{\mathbf{r}} = x + (y - 1)L_x$$

Let me break this through. For each site $\mathbf{r}$, two sequential indices are provided ($2j_{\mathbf{r}} - 1$, hosting spin $\uparrow$, and $2j_{\mathbf{r}}$, hosting spin $\downarrow$). $j_{\mathbf{r}}$ just orders the site rows-wise. This way, $(x, 1)$ is assigned to $j_{(x,1)} = x$, while its NN one site above $(x, 2)$ is assigned to an entry shifted by L_x, $j_{(x,2)} = x + L_x$. This is just a way of counting the site of a finite square lattice by sweeping along a row and then moving to the row above. Fig. A.7 reports a scheme of the used site ordering.

Within this convention, matrix elements $H_{\alpha\beta}$ are defined by:

- If $\sigma = \sigma'$ and $\mathbf{r}$, $\mathbf{r}'$ are NN, the matrix entry is $-t$. In terms of the used greek indices, α and β satisfy said requirement if $|\alpha - \beta| = 2$ (horizontal hopping) or $|\alpha - \beta| = 2L_x$ (vertical hopping). Along column α of the hamiltonian matrix, the elements $-t$ appear at positions

$$(\alpha \pm 2L_x) \mod D \quad \text{and} \quad (\alpha \pm 2) \mod D$$

- If $\mathbf{r} = \mathbf{r}'$ and $\sigma = \sigma'$ (along the diagonal), the local interaction with the mean field is given by the matrix element

$$-mU \times (-1)^{x+y} \times (-1)^{\delta_{\sigma = \downarrow}}$$

Starting from a given entry α, $j_{\mathbf{r}}$ is retrieved simply by $j_{\mathbf{r}} = \lfloor \alpha/2 \rfloor$, and then

$$x + y = (j_{\mathbf{r}} + 1) - \left\lfloor \frac{j_{\mathbf{r}}}{L_x} \right\rfloor (L_x - 1)$$

Then the $j_{\mathbf{r}}$-th 2×2 block along the diagonal will be given by

$$(-1)^{x+y} \underbrace{\begin{bmatrix} -mU & \\ & mU \end{bmatrix}}_{\mathcal{B}}$$

Note that the resulting block diagonal contribution to the hamiltonian is shaped like follows (assume L_x to be even):

$$
\begin{array}{c}
\begin{array}{ccccccc}
\color{red}1 & \color{red}2 & \color{red}\cdots & \color{red}L_x - 1 & \color{red}L_x & \color{red}L_x + 1 & \color{red}L_x + 2 & \color{red}\cdots
\end{array} \\
\begin{array}{c}
\color{red}1 \\ \color{red}2 \\ \color{red}\vdots \\ \color{red}L_x - 1 \\ \color{red}L_x \\ \color{red}L_x + 1 \\ \color{red}L_x + 2 \\ \color{red}\vdots
\end{array}
\begin{bmatrix}
\mathcal{B} & & & & & & \\
& -\mathcal{B} & & & & & \\
& & \ddots & & & & \\
& & & \mathcal{B} & & & \\
& & & & -\mathcal{B} & & \\
& & & & & -\mathcal{B} & \\
& & & & & & \mathcal{B} \\
& & & & & & & \ddots
\end{bmatrix}
\end{array}
$$

Along the same row, on the diagonal the 2×2 blocks $\mathcal{B}$ alternate signs; changing row (in the example above, at positions $L_x, L_x + 1$), due to the anti-ferromagnetic configuration of local mean-fields, an additional -1 is included. If L_x is taken to be odd, the diagonal blocks just alternate signs all the way.

These prescriptions allow to build from scratch the hamiltonian matrix. After that, diagonalization provides D orthonormal eigenvectors $\mathbf{v}^\ell \in \mathbb{C}^{D \times D}$ with $\ell = 1, \cdots, D$, each associated to a precise eigenvalue $\epsilon^\ell \in \mathbb{R}$. At equilibrium, electrons will fill up the energy eigenstates according to,

$$\langle \hat{n}_{\mathbf{r}\sigma} \rangle = \sum_{\ell=1}^{D} |v_\alpha^\ell|^2 f(\epsilon^\ell; \beta, \mu) \quad \text{where} \quad \alpha = (\mathbf{r}\sigma)$$

For a fixed filling $n = N/D$, the chemical potential must satisfy

$$
\begin{aligned}
n &= \frac{1}{D} \sum_{\mathbf{r}\sigma} \langle \hat{n}_{\mathbf{r}\sigma} \rangle \\
&= \frac{1}{D} \sum_{\mathbf{r}\sigma} \sum_{\ell=1}^{D} |v_\alpha^\ell|^2 f(\epsilon^\ell; \beta, \mu) \\
&= \frac{1}{D} \sum_{\ell=1}^{D} f(\epsilon^\ell; \beta, \mu)
\end{aligned}
$$

since the $\mathbf{v}^\ell$ eigenvectors are orthonormal. The chemical potential for the half-filled model is already known to be

$$\mu\big|_{n=1/2} = -\frac{U}{2}$$

as evident from Eq. (A.3). Average magnetization is then given by

$$
\begin{aligned}
m &= \frac{1}{D} \sum_{\mathbf{r}} (-1)^{x+y} \left[\langle \hat{n}_{\mathbf{r}\uparrow} \rangle - \langle \hat{n}_{\mathbf{r}\downarrow} \rangle \right] \\
&= \frac{1}{D} \sum_{\lambda=1}^{D/2} (-1)^{(\lambda+1) - \lfloor \lambda/L_x \rfloor (L_x - 1)} \sum_{\ell=1}^{D} \left[\left| v_{2\lambda-1}^\ell \right|^2 - \left| v_{2\lambda}^\ell \right|^2 \right] f(\epsilon^\ell; \beta, \mu)
\end{aligned}
\tag{A.19}
$$

since $\mathbf{r}\uparrow$ is associated to an odd index entry, while $\mathbf{r}\downarrow$ to the following even entry. The associated HF algorithm is identical to the one presented in Sec. A.3.7, with the following substitutions:

2. Initialize the hamiltonian matrix $H_{\alpha\beta}$ matrix according to the initialized m_0 and the site indexing rules of Fig. A.7;

4. Diagonalize the matrix associated to the operator $\hat{H}_{\alpha\beta} - \mu \hat{N}$ collecting the $\mathbf{v}^\ell$ eigenvectors;

5. Compute m using Eq. (A.19) and update the counter, $i \to i+1$;

A.4   (Impossibility of) BCS-like superconducting phase

[To be continued...]